



NRC Publications Archive Archives des publications du CNRC

A novel platform for engineering blood-brain barrier-crossing bispecific biologics

Farrington, Graham K.; Caram-Salas, Nadia; Haqqani, Arsalan S.; Brunette, Eric; Eldredge, John; Pepinsky, Blake; Antognetti, Giovanna; Baumann, Ewa; Ding, Wen; Garber, Ellen; Jiang, Susan; Delaney, Christie; Boileau, Eve; Sisk, William P.; Stanimirovic, Danica B.

This publication could be one of several versions: author's original, accepted manuscript or the publisher's version. / La version de cette publication peut être l'une des suivantes : la version prépublication de l'auteur, la version acceptée du manuscrit ou la version de l'éditeur.

For the publisher's version, please access the DOI link below. / Pour consulter la version de l'éditeur, utilisez le lien DOI ci-dessous.

Publisher's version / Version de l'éditeur:

<https://doi.org/10.1096/fj.14-253369>

The FASEB Journal, 28, 11, pp. 4764-4778, 2014-07-28

NRC Publications Record / Notice d'Archives des publications de CNRC:

<https://nrc-publications.canada.ca/eng/view/object/?id=710861bf-e0dc-46d5-a21b-110ea6a6997b>

<https://publications-cnrc.canada.ca/fra/voir/objet/?id=710861bf-e0dc-46d5-a21b-110ea6a6997b>

Access and use of this website and the material on it are subject to the Terms and Conditions set forth at

<https://nrc-publications.canada.ca/eng/copyright>

READ THESE TERMS AND CONDITIONS CAREFULLY BEFORE USING THIS WEBSITE.

L'accès à ce site Web et l'utilisation de son contenu sont assujettis aux conditions présentées dans le site

<https://publications-cnrc.canada.ca/fra/droits>

LISEZ CES CONDITIONS ATTENTIVEMENT AVANT D'UTILISER CE SITE WEB.

Questions? Contact the NRC Publications Archive team at

PublicationsArchive-ArchivesPublications@nrc-cnrc.gc.ca. If you wish to email the authors directly, please see the first page of the publication for their contact information.

Vous avez des questions? Nous pouvons vous aider. Pour communiquer directement avec un auteur, consultez la première page de la revue dans laquelle son article a été publié afin de trouver ses coordonnées. Si vous n'arrivez pas à les repérer, communiquez avec nous à PublicationsArchive-ArchivesPublications@nrc-cnrc.gc.ca.



A novel platform for engineering blood-brain barrier crossing bispecific biologics

Graham K. Farrington^{1*†}, Nadia Caram-Salas², Arsalan S. Haqqani², Eric Brunette², John Eldredge¹, Blake Pepinsky¹, Giovanna Antognetti¹, Ewa Baumann², Wen Ding², Ellen Garber¹, Susan Jiang², Christie Delaney², Eve Boileau², William Sisk¹, Danica B. Stanimirovic^{2*†}

¹Biogen Idec Inc, 12 Cambridge Center, Cambridge, MA 02142.

²Human Health Therapeutics Portfolio, National Research Council of Canada, Ottawa, ON K1A0R6.

*To whom correspondence should be addressed:

Graham.farrington@biogenidec.com

† 12 Cambridge Center, Cambridge, MA 02142

Tel: 1-617-679-3224

Danica.stanimirovic@nrc-cnrc.gc.ca

† 1200 Montreal Road, Building M54, Ottawa, ON K1A0R6

Tel: 1-613-993-3730

Fax: 1-613-941-4475

Running title:

Blood-brain barrier crossing antibodies

Abbreviations:

ADCC: Antibody-dependent cell-mediated cytotoxicity

AUC: Area under the curve

BBB: Blood-brain barrier

BEC: Brain endothelial cells

CDR: Complementary determining region

CHO: Chinese hamster ovary

CFA: Complete Freund's adjuvant

CMV: Cytomegalovirus

CSF: Cerebrospinal fluid

DTT: Dithiotreitol

FACS: Fluorescent-activated cell sorting

FCS: Fetal calf serum

GDNF: Glial-derived neurotrophic factor

HEPES: 4-(2-hydroxyethyl)-1-piperazineethanesulfonic acid

icv: intracerebroventricular

IgG: Immunoglobulin G

IR: Insulin receptor

ISF: Interstitial fluid

iv: Intravenous

kDa: Kilodalton

K_d_{app}: Apparent affinity

LRP: Low-density lipoprotein related protein

MOR: mu opioid receptors

MPE: Maximal possible effect

MRM: Multiple reaction monitoring

nanoLC MS/MS: nanoflow liquid chromatography tandem mass spectrometry

NGS: Normal goat serum

NIH: National Institutes of Health

NPY: Neuropeptide Y

PBS: Phosphate buffered saline

PK/PD: Pharmacokinetics/pharmacodynamics

RMT: Receptor-mediated transcytosis

SEC: Size-exclusion chromatography

SMCC: Sulfo-succinimidyl4-[N-maleimidomethyl]cyclohexane-1-carboxylate

SRM: Selected reaction monitoring

ILIS: isotopically labeled internal standard

SV-ARBEC: Simian virus 40-immortalized adult rat brain endothelial cells

TfR: Transferrin receptor

V_HH: Camelid single-domain antibody

Abstract:

The blood-brain barrier (BBB) prevents the access of therapeutic antibodies to CNS targets. The engineering of bispecific antibodies in which a therapeutic 'arm' is combined with a blood-brain barrier transcytosing 'arm' can significantly enhance their brain delivery. The BBB-permeable single-domain antibody FC5, was previously isolated by phenotypic panning of a naïve llama single domain antibody phage display library. In this study, FC5 was engineered as a mono- and bivalent fusion with the human Fc domain to optimize it as a modular brain delivery platform. *In vitro* studies demonstrated that the bivalent fusion of FC5 with Fc increased the rate of transcytosis (P_{app}) across brain endothelial monolayer by 25% compared to mono-valent fusion. Up to a 30-fold enhanced apparent brain exposure (derived from serum and cerebrospinal fluid pharmacokinetic profiles) of FC5- compared to control domain antibody-Fc fusions after systemic dosing in rats was observed. Systemic pharmacological potency was evaluated in the Hargreaves model of inflammatory pain using the blood-brain barrier-impermeable neuropeptides Dalargin and Neuropeptide Y chemically conjugated with FC5-Fc fusion proteins. Improved serum pharmacokinetics of Fc-fused FC5 contributed to a 60-fold increase in pharmacological potency compared to the single-domain version of FC5; bivalent and mono-valent FC5 fusions with Fc exhibited similar systemic pharmacological potency. The study demonstrates that modular incorporation of FC5 as the BBB-carrier arm in bi-specific antibodies or antibody-drug conjugates offers an avenue to develop pharmacologically active biotherapeutics for CNS indications.

Key words:

Blood-brain barrier; Single-domain antibody; Neuropeptides; Drug delivery; Bi-specific biologics

Introduction

Therapeutic antibodies have become a dominant drug-developing pipeline for treatment of oncology and inflammatory diseases. However, the development of therapeutic antibodies for CNS indications is hindered by the BBB, which prevents passive diffusion of hydrophilic molecules >400 Da from the blood into the brain parenchyma and excludes virtually all protein therapeutics (1).

The capillary bed in the brain is composed of a tight-junction-connected endothelial cell layer which, through anatomical and functional interactions with pericytes, astrocytic end-feet and perivascular neurons, forms the neurovascular unit (2). Brain capillaries contain various efflux and directional transporters that actively establish transportation gradients across the BBB (1, 3). The restrictive physical and functional barriers prevent the entrance of both adverse agents, including toxins and viruses, as well as therapeutic entities. Therefore, the development of biotherapeutics targeting the CNS is tied to the development of BBB delivery methods (4).

Delivery of macromolecules important for brain function can be achieved by the receptor-mediated transcytosis (RMT) across the BBB (4–6). RMT is initiated by a ligand binding to the endothelial receptor presented on the luminal (blood) surface followed by ligand/receptor complex internalization, endosomal sorting, subsequent ligand release on the abluminal endothelial surface and receptor recycling back to the luminal membrane (5). Examples of these physiological shuttles include the transferrin receptor (TfR) (7), insulin receptor (IR) (8), and receptors involved in trafficking of lipid ligands (LRP family) (9). They have been used as Trojan horses to ‘piggy-back’ therapeutic macromolecules across the BBB.

Examples of the application of this approach include the use of antibodies to the transferrin receptor (7) and insulin receptor (10, 11). Unfortunately, these RMT targets are highly and broadly expressed in tissues and are implicated in metabolically critical cellular functions creating safety risks as recently reported (12, 13).

Antibodies targeting alternative RMT pathways are sought to facilitate the development of BBB penetrating biotherapeutics. One such antibody, FC5, has been isolated by phenotypic screening of camelid single-domain antibody library for BBB-crossing antibodies (14). FC5 engages active RMT process by binding epitopes of the BBB-enriched transporter (15) conserved in human, mouse and rat and has been detected in CSF and brain parenchyma of rodents by targeted mass spectroscopy, imaging and immunofluorescence (16, 17). The objective of this study was to establish whether FC5 can be optimized as a modular BBB delivery platform. FC5 was evaluated in mono- or bivalent fusions with human Fc domain in *in vitro* and *in vivo* models. The objective of *in vitro* studies was to determine the effects of apparent affinity ($K_{d_{app}}$) and valency of FC5 on the rate of transcytosis (P_{app}); the objective of *in vivo* studies in rats was to establish a role of plasma pharmacokinetics, $K_{d_{app}}$ and valency of FC5 binding in apparent CNS exposure and pharmacological responses elicited through the engagement of CNS target receptors. Plasma half-life and affinity-optimized FC5 fused with Fc domain in either mono- or bivalent manner markedly enhanced brain exposure and pharmacological potency in the CNS of FC5-Fc-neuropeptide conjugates, suggesting that modular incorporation of FC5 as BBB-carrier arm provides a platform to increase therapeutic concentrations in the CNS and that it can be used in the development of CNS-targeted biotherapeutics.

Methods and Protocols

Expression, purification and biophysical characterization of V_HHs and their fusions with Fc domain

The molecules (V_HHs and V_HH-Fc-fusions) used in this study and their characteristics are summarized in the Table 1.

Camelid V_HHs FC5, EG2 and A20.1 were expressed, purified and characterized as described in detail previously (15, 18). FC5 and EG2 V_HHs were expressed in fusion with His5 and c-myc tags, while A20.1 was expressed with His6 and c-myc tag to allow for purification by immobilized metal affinity chromatography using HiTrap Chelating™ column and for detection by immunochemistry, respectively.

The camelid V_HHs were fused to the N- or C- terminus of an aglycosyl human IgG1 Fc and hinge (human IgG1 E216-K447, T299A mutation kabat numbering) or to the N-terminus of a human single chain Fc and hinge (19) the consensus N-glycosylation sites Asn-Xaa-Ser/Thr in Fc were altered to Asn-Xaa-Ala to prevent glycosylation in all fusions. In some cases, V_HHs were fused to the N-terminus of the mouse Fc and hinge domain (mouse IgG2a) instead of human (Table 1) to allow for paired quantification of V_HH-hFc and V_HH-mFc after co-administration. DNA constructs were cloned into a CMV promoter driven expression vector. N-terminal leader sequences for expression was MDWTWRVFCL LAVAPGAHS for all FC5 sequences fused N or C-terminally to the human Fc or mouse Fc domain. Plasmid was transfected into CHO DG44 cells and selected for stable integration using standard techniques. Cells were cultured in suspension with rotation in shake flasks at 120-140 rpm, 5% CO₂, 37°C, at a density of 5-8 x10⁶/ml, cells were growth-arrested by reducing the temperature to 28°C and held in culture for an additional 10-14 days or until the cell viability dropped below

70%. Conditioned media was clarified by centrifugation followed by 1 μ m and 0.2 μ m filtration. Proprietary expression vector, CHO cells and serum-free media were utilized.

Fusion proteins were purified from clarified and filtered culture medium on recombinant Protein A Sepharose Fast Flow (GE Healthcare, Chalfont St. Giles, Buckinghamshire, UK) at 10 mg of mAb/ml of resin, then concentrated in a Vivaspin 5kDa (Vivaproducts, Littleton, MA), and chromatographed on a Superdex-200 (2.6 x 87 cm) column (GE Healthcare) to eliminate protein aggregates. Endotoxin levels were determined using the Endosafe System (Charles River, Charleston, SC) and were less than 1.0 EU/mg of protein.

Samples were subjected to SDS-PAGE on 4-12% Bis-Tris NuPAGE gradient gel (Invitrogen, Carlsbad, CA). Non-reduced samples were treated with 5 mM N-ethyl maleimide for 5 min at room temperature then diluted with Invitrogen non-reducing sample buffer, heated at 95°C for 2 min and electrophoresed. Reduced samples were treated with sample buffer containing 2% 2-mercaptoethanol and heated as above.

Size exclusion chromatography was carried out on a Phenomenex BioSep SEC s3000 column 300 x 7.8 mm (Torrance, CA) in 20 mM sodium phosphate pH 7.2, 150 mM NaCl (PBS) at a flow rate of 0.6 ml/min using a Waters Alliance instrument (Millipore, Milford, MA). In addition to UV detection, the eluent was monitored with an Optilab Rex refractive index detector (Wyatt, Santa Barbara, CA). Light scattering was monitored using a Treos MiniDawn detector (Wyatt). Molecular weight of each complex was determined using the Wyatt Astra Software.

Conjugation of V_HHs and their Fc fusions with neuroactive peptides

The V_HHs and V_HH-Fc fusions were conjugated to the hexapeptide leu-enkephalin analog Dalargin having the sequence Tyr-dAla-Gly-Phe-Leu-Arg-cysteamide (Biomatic Corp, Cambridge, ON).

Peptides were conjugated using the general method as described by Mattson et al (20) using SMCC (Pierce Rockland, IL). Briefly, SMCC (10 mg/mL) in N,N-dimethylformamide was added in 7.5 fold molar excess to the target antibody, at 1-2 mg/ml, in PBS. The reaction was incubated for 2.5 h at room temperature and Dalargin-Cys in 50 mM MES pH 6.0 was added in a 4 fold molar excess to the SMCC. The Dalargin-labeled protein was concentrated in a Vivaspin 5kDa devices, and chromatographed on a superdex 75 (2.6 x 87 cm) column (GE Healthcare) to separate unlinked Dalargin and hydrolyzed SMCC from Dalargin-SMCC labeled antibody.

The stoichiometry of Dalargin linked molecules per fusion protein was determined from the intact mass spectrometry distribution of labeled proteins. Each of the Dalargin-coupled molecules was deglycosylated with PNGase F and reduced overnight with DTT; then, ~50 picomoles of the reduced polypeptides were purified using a C₄ MacroTrap™ 3x8 mm cartridge (Bruker, Billerica MA), analyzed on an LCT Premier 3 mass spectrometer; the intact molecular mass of each polypeptide was deconvoluted with the MaxEnt-1 program. The number of Dalargins linked to each protein sequence was determined from the protein mass plus the linker and peptide mass.

Quantitative analytics for V_HHs and V_HH-Fc fusion proteins

V_HH and V_HH-Fc protein levels in cell media and serum and CSF were quantified using ELISA and/or targeted nanoLC MS/MS.

ELISA: Costar 96-well easy wash plates (Corning Life Sciences, Lowell, MA) were coated with 5 µg/ml anti-hFc (50 µl/well), in 50 mM sodium carbonate, pH 9.5, overnight at 4°C. All subsequent steps were carried out at room temperature and included four washes with PBS plus 0.05% Tween 20 between steps. Plates were blocked for 1 h with 1% bovine serum albumin, 0.1% ovalbumin, and 0.1% nonfat dry milk in Hank's balanced salt buffer plus 25 mM HEPES, pH 7.0, incubated for 1 h with 3-fold serial dilutions of test samples in blocking solution as above containing 25 mM HEPES, pH 7.0, then incubated for 1 h with donkey anti-human F(ab)-alkaline phosphatase (Jackson ImmunoResearch Laboratories Inc., West Grove, PA) in sample 1% BSA, 0.05% Tween 20, PBS. Wells were then treated with 10 mg/ml 4-nitrophenylphosphate alkaline phosphatase substrate in 100 mM glycine, pH 10.5, 1 mM MgCl₂, and 1 mM ZnCl₂. Plates were read at 405 nm using a Molecular Devices (Sunnyvale, CA) plate reader.

nanoLC/MS/MS: Pure V_HH or V_HH-Fc fusion proteins, *in vitro* BBB transport- or body fluid samples containing these proteins were reduced, alkylated and trypsin digested using previously described protocol (16, 21). For ILIS-based quantification, isotopically heavy versions of the peptides that contained heavy C-terminus K (+8 Da) were synthesized from a commercial source (New England Peptide LLC, Gardner, MA) (22). Each protein was first analyzed by nanoLC-MS/MS using data-dependent acquisition to identify all ionizable peptides and the 3 to 5 most intense fragment ions were chosen. An initial SRM assay was developed to monitor these fragments at attomole amounts of the digest. Fragments that showed reproducible intensity ratios at low amounts (about 100-300 amol; Pearson $r^2 \geq 0.95$) were considered stable and were chosen for the final SRM assay (see Table 1). The location of peptides chosen for SRM with

respect to CDR regions of antibodies is shown in Fig S3. The blood contamination of CSF samples was evaluated by 'in-reaction' monitoring of albumin levels using a nanoLC-SRM method as described previously (16). A percentage of above 0.07% serum albumin was considered blood contaminated CSF and was excluded from further analyses.

Cell binding of V_HH-Fc fusions: FACS Assays and Analysis

SV-ARBEC, established by SV-40 transfection of primary rat BEC isolated from 24-30 days old Sprague-Dawley rats (23) were used for cell binding assays and for *in vitro* BBB permeability assays.

SV-ARBEC cells were resuspended in 1% heat inactivated FCS 1x PBS (FACS buffer) at 500,000 cells/ml, and 100 μ l of the cell suspension was mixed in a 96-well V bottom polypropylene plate (Nunc) with 100 μ l of V_HH-Fc fusion molecules in the same buffer. After one-hour incubation at 4°C, pelleted cells were washed three times and then resuspended in 100 μ l Goat anti-human IgG Fc – PE (Jackson ImmunoResearch Labs, West Grove, PA), diluted 1/300 in FACS buffer, incubated 1h at 4°C, centrifuged at 1200rpm for 3 min; cell pellets were washed, fixed with 150 μ l/well 1% paraformaldehyde for 10 min at room temperature, centrifuged, the fix solution was decanted and cell pellets were resuspended in 175 μ l FACS buffer for analysis. Cellular fluorescence was determined on FACScan equipped with Cellquest software (Becton-Dickinson, Franklin Lakes, NJ). The data were plotted as a function of mean channel fluorescence versus the concentration. The K_d_{app} values were determined by fitting the data with a single site total binding model using GraphPad Prism 6.0 (LaJolla, CA).

***In vitro* BBB model and permeability studies**

SV-ARBECS were seeded at 80,000 cells/membrane on rat-tail collagen coated 0.83 cm² Falcon cell inserts, 1 µm pore size in 1 ml SV-ARBECS feeding media without phenol red. The model characterization is described in detail in Garberg et al (23). The wells of a 12-well tissue culture plate (i.e., bottom chamber) contained 2 ml of 50:50 (v/v) mixtures of SV-ARBECS media without phenol red and rat astrocyte-conditioned media. The model was used when $P_{e[\text{sucrose}]}$ was between 0.4-0.6 [$\times 10^{-3}$] cm/min. Transport experiments were performed exactly as described in Haqqani et al. (16) by adding a mixture of V_HHs or their Fc fusions in equimolar concentrations to the top chamber and by collecting the 100 µl aliquots (with subsequent replacement with 100 µl of transport buffer) from the bottom chamber at 15, 30, 60 and 90 min for simultaneous quantification of all antibodies using multiplexed SRM-ILIS method. The apparent permeability coefficient P_{app} was calculated as described previously (24).

Animal experiments

Male Wistar rats aged 8-10 weeks (weight range, 230–250 g) were used for intracisternal cannulation or intracerebroventricular (icv) or intravenous (iv) administrations of various antibodies. All animals were purchased from Charles River Laboratories International, Inc. (Wilmington, MA, USA). Animals were housed in groups of three in a 12 h light/dark cycle at a temperature of 24°C and a relative humidity of 50 ± 5% and were allowed free access to food and water. All animal procedures were approved by the National Research Council of Canada's Animal Care Committee and were in compliance with the Canadian Council of Animal Care guidelines.

Serum/CSF Pharmacokinetics

Cisterna magna cannulation: The technique for multiple sampling of cisterna magna CSF was developed from different methods previously described (25, 26) by introducing several modifications. This modified technique does not involve drilling through the skull, as described by other methods, avoiding damage of the meninges and the adjacent nervous tissue.

Rats were anaesthetized with a ketamine/xylazine mixture (45/12 mg/kg, intraperitoneal) and mounted in a stereotaxic instrument (Kopf, model 900, Tujunga, CA, USA). An incision beginning at a line joining the ears and extending about 3 cm in a caudal direction was made in the midline: the fascia and neck muscles were retracted exposing the atlanto-occipital membrane; the rat's head was then rotated downward to about 45° angle and a small hole was made using the tip of a 27G disposable needle; polyethylene tubing (PE-20) was then inserted 0.5 cm into the slit. The cannula was fixed to the atlanto-occipital membrane with Histoacryl glue and then flushed thoroughly with artificial CSF. The free part of the cannula (4-5 cm) was threaded through the skin with a 20G needle, the muscle and the skin were closed, the exposed portion was cut to desired length and the tip was slightly heated to prevent backflow of CSF. The animal was placed in a recovery room for five days to allow the closing of the cisterna magna.

Serial plasma and CSF collection: CSF and blood samples were collected at different times (0.25, 0.5, 1, 4, 24, 48, 72 and 96 h) after the tail vein administration of compounds. For CSF collection, rats were briefly and lightly anesthetized with 3% isoflurane, and 5 µl of CSF was collected from the collecting portion of the cannula by inserting a 30Ga needle attached to an insulin syringe; the samples were stored at -80°C until analysis. In some instances, CSF was collected at discrete time points as described previously (16, 27). Blood samples were taken at

the same time points as CSF from the tail vein according to Fluttert et al. (28) using a polymer gel tubes (Becton, Dickinson and Company, Franklin Lakes, NJ USA). Samples were centrifuged (15 min at 15,000 g; room temperature) and serum was stored at -80 °C until analysis. Antibody levels in paired serum and CSF samples were quantified by targeted nanoLC MS/MS. Blood and CSF pharmacokinetic analyses were performed using WinLin 6.0 program. Apparent CNS exposure was estimated from the ratio of $AUC_{[CSF]}/AUC_{[serum]}$ levels over 96 h.

***In Vivo* Target Engagement Studies**

The potencies of V_HH and V_HH-Fc fusion proteins chemically cross-linked with Dalargin in suppressing thermal hyperalgesia in Hargreaves model of inflammatory pain were compared following icv or systemic administration.

For icv administration, the animals were anaesthetized using 2 to 4% isoflurane and mounted in a stereotactic instrument (Kopf, model 900, Tujunga, CA, USA). The fur of the head was shaved and skin incision approximately 15 mm long was made to localize the Bregma line. A 25G needle attached to a Hamilton 10 µl syringe (Hamilton Co., Reno, NV) with a PE-20 polyethylene tube filled containing sterile water was inserted using the coordinates described by Paxinos et al. (29); -0.8 mm anterior/posterior to Bregma, 1.5 mm lateral from midline and 3.5 mm through the skull (dorsal/ventral) to administer the compounds. After the administration of compounds, the needle was kept in place for 5 min to minimize backflow, the hole in the bone was closed with sterile bone wax and the skin was sutured. All injections were given in a volume of 5 µl over 5 minutes (rate of 1 µl/min).

Hargreaves model of inflammatory hyperalgesia: Chronic inflammatory hyperalgesia was induced by injecting a low volume (100 μ l) of complete Freund's adjuvant (CFA; heat-killed *M.tuberculosis*; Sigma, St. Louis, MO) suspended in oil:saline 1:1 emulsion into a right paw (59). The paw withdrawal latency in response to the application of a radiant stimulus onto the plantar surface of both right and left paw was measured using the plantar Analgesia Meter equipment for paw stimulation (IITC Life Science, Woodland Hills, CA). To avoid heat-sink, the temperature of the glass plate was maintained at $29\pm 1^{\circ}\text{C}$; the intensity of the radiant heat light source was adjusted to 20%, resulting in approximate temperature of 60°C . The time taken by the animal to respond by licking or flicking its paw was interpreted as a positive response (paw withdrawal latency). A cut-off time (20 s) was established at the end of which the heat source shuts off automatically to avoid tissue damage.

Two days prior to CFA injection the light-intensity lamp was adjusted to elicit baseline paw withdrawal latencies between 17-20 s in both paws for each animal. Two days after CFA injection and prior to the administration of antibodies, the baseline was measured again in both paws to confirm the development of thermal hyperalgesia; the non-inflamed paw was always used as control. Animals with latency times greater than 6s in "inflamed paw" and less than 17s in "normal paw" were excluded from the further experiment.

Animals were randomized (one per cage) and staff performing pain experiments were blinded to the randomization and the content of injectable compounds. On the day of the experiment, the animals were acclimatized in the analgesia meter equipment for at least 30 min. For V_{HH} -neuropeptide conjugates, rats received 1-3 iv injections (through tail vein; one hour apart) of PBS, Dal-cystaemide, FC5, FC5-Dal, EG2, EG2-Dal and FC5 with free Dal-Cystaemide, or 5 μ l icv injection of the same molecules. Fc-fusion molecules were given in one

iv. injection at varying concentrations (0.5, 2.5, 6 and 21 mg/kg) in a volume no higher than 1 ml per animal. The paw (inflamed and control) withdrawal latency was measured at 15 min intervals over 3-6 h.

All results were presented as means \pm SEM for 3-5 animals per group (based on evaluation of variation coefficient in pre-study experiments). The AUC was calculated by trapezoidal method to derive %MPE using the following formula:

$$\%MPE = [(AUC \text{ molecule} - AUC \text{ inflamed paw}) / (AUC \text{ normal paw} - AUC \text{ inflamed paw})] \times 100,$$

where AUC inflamed paw and AUC normal paw are the values obtained from the group injected with the vehicle (PBS). One-way ANOVA, followed by the Tukey's test, was used to compare differences between treatments in behavioral experiments. Differences were considered to reach statistical significance when $P < 0.05$.

Detection of antibodies in brain sections

Rat brains were perfused with 20 ml saline supplemented with 1EU/ml Heparin (Organon, Toronto, ON) at 2ml/min and harvested at various times after tail-vein injection of FC5 fusion proteins (e.g., Bi-FC5-hFc) or control antibodies. Brains were frozen and sectioned on a cryostat into 12 μ m sections. Sections were fixed for 10 min at room temperature in 100% methanol, washed 3 times in PBS and incubated in 10% normal goat serum (NGS) containing 0.3% Triton X-100 in PBS for 1h. After washing 3 times in PBS, goat anti-human Fc (Jackson Immuno Research) 1:500 in 5% NGS containing 0.3% Triton X-100 in PBS was applied overnight at 4°C. Sections were washed 3 times in PBS and incubated with mouse-anti-rat NeuN antibody (ABCAM, Toronto, ON) 1:100 in 5% NGS/PBS for 1 h at room temperature. After

washing, sections were incubated in 1:300 goat anti-mouse Alexa 647 (Invitrogen, Burlington, ON) in PBS. Vasculature-staining fluorescent lectin RCAI (Vector Laboratories, Burlington, ON) 1:500 in PBS was then added for 10 min. After washing in PBS, sections were covered in Dako fluorescent mounting medium (Dako, Burlington, ON) spiked with 2 $\mu\text{g/mL}$ Hoechst (Invitrogen) to stain nuclei. Images were captured with Olympus 1X81 Fluorescent Microscope using 10X and 60X objectives.

Results

Design and biophysical characterization of FC5 fusion proteins

The single-domain antibodies (V_{HH} s) and V_{HH} -Fc fusion proteins used in the study are shown in Table 1 and schematically in Fig. 1A. Each molecule was characterized on SDS PAGE and by analytical SEC-LS to confirm homogeneity and lack of aggregates. Purified molecules exhibited the expected banding patterns by SDS PAGE (Fig. 1B) and showed single peaks by SEC with the expected molecular weight corresponding to each molecule (not shown).

Antibodies (V_{HH} s or V_{HH} -Fc fusions) were conjugated with BBB-impermeable neuropeptides Dalargin or neuropeptide Y using the bifunctional crosslinker SMCC. The number of peptides crosslinked was determined by mass spectrometry and was optimized to achieve an average of 1.5 peptides linked to each molecule (Table S1).

Binding affinity of V_{HH} s and their Fc fusion variants

The dimerization of V_HH fragments through an Fc fusion enhances antibody binding affinity due to increased avidity ($K_{d_{app}}$). The binding of bivalent Bi-FC5-hFc, monovalent Mono-FC5-hFc and irrelevant control V_HH-hFc (no data shown) fusion proteins to SV-ARBEC was examined by FACS analysis. While monovalent FC5 fused to the N-terminus of single chain Fc (Mono-FC5-hFc) showed insufficient binding to SV-ARBEC cells to calculate a $K_{d_{app}}$ due to the rapid dissociation of the monomeric construct during the cellular washes (Fig. 2A), the Bi-FC5-hFc showed saturable binding (Fig. 2A) with $K_{d_{app}}$ of 46 ± 5 nM. FC5 fused to hFc in C-terminal configuration (hFc-Bi-FC5) showed significantly attenuated binding to SV-ARBEC compared to Bi-FC5-hFc (Fig. 2A).

***In vitro* BBB permeability of V_HHs and their Fc fusion variants**

The rate of transport of V_HHs and their Fc fusion variants across *in vitro* BBB model was determined as previously described (15, 16). The molecules were co-applied to the upper chamber of the *in vitro* BBB model in various paired or multiplexed combinations and quantified by SRM in the bottom compartment; P_{app} value for each was calculated over 90 min. The (top chamber) input concentration of Bi-FC5-hFc was between 1.5 and 3 μ M (linear phase) with equimolar input of various co-administered control antibodies.

Comparison of *in vitro* P_{app} values of FC5 and its hFc fusion designs in experiments paired with controls is shown in Fig. 2B. Control molecules of various molecular weights, 12.5 kDa, V_HH EG2 and 150 kDa, anti-HEL IgG, showed similar low P_{app} values ranging between $5-8 \times 10^{-6}$ cm/min; in contrast P_{app} values for FC5 (in over 50 separate experiments) were $116.4 \pm 32.9 \times 10^{-6}$ cm/min. N-terminally fused Bi-FC5-hFc demonstrated 80% higher P_{app} than FC5,

while P_{app} for Mono-FC5-hFc was similar to that of FC5 (Fig. 2B). Bivalent C-terminally fused hFcFC5 had a much lower P_{app} value than either FC5 or Bi-FC5hFc and no significant increase relative to the negative controls, suggesting 'loss of BBB transport function' in this linkage configuration.

Plasma and CSF pharmacokinetics of V_HH -Fc fusion variants

V_HH domains (15 kDa), including FC5, are subject to kidney filtration and have short serum pharmacokinetic (PK) half-lives (β -phase $t_{1/2}$ 25 min) (17). Conversely, FC5 fused to Fc exhibited a significant prolongation of the circulation half-life; Bi-FC5-hFc, Mono-FC5-hFc and the hFc domain alone had similar beta-phase half-lives (45 h, 64 h, and 55 h, respectively), suggesting that when these molecules are dosed at the same concentrations they should have equal exposure to the BBB.

After systemic co-administration of short half-life FC5 and control V_HH s A20.1 or EG2, only FC5 was detected in the CSF (CSF/serum ratio of 0.2% 2 h after injection) (16). To estimate CNS exposure for the Fc fusions with much longer serum half-life, a serial collection of blood and cisterna magna CSF was performed over 96 h in animals co-administered with Bi-FC5-hFc and Bi-A20.1-mFc (each at 6 mg/kg iv). Antibody levels were determined by a sensitive SRM-ILIS method, allowing quantitative measurement in small volumes ($\sim 5 \mu\text{l}$) of serially collected CSF as well as 'in-reaction' monitoring for blood contamination by calculating CSF/serum albumin ratios. Serum/CSF PK profiles of Bi-FC5-hFc and Bi-A20.1-mFc in the same animals and CSF/serum ratio for each molecule are shown in Fig. 3A. Whereas serum PK

profiles of Bi-FC5-hFc and Bi-A20.1-mFc were similar (Fig. 3A, upper panel) yielding $t_{1/2}$ of 22 ± 5 h and 25 ± 8 h, respectively, CSF levels of Bi-FC5-hFc were significantly higher from Bi-A20.1-mFc levels, reaching maximum (~ 200 ng/ml) 24 h after dosing for Bi-FC5-hFc versus (10ng/ml) for Bi-A20.1-mFc (Fig. 3A, middle panel). Bi-A20.1-mFc had a low CSF/serum ratio ranging from 0.001 to 0.08%, whereas the Bi-FC5-hFc CSF/serum ratio profile plateaued at $\sim 1\%$ between 24 and 48 h after injection (Fig. 3A, bottom panel). To estimate apparent CNS exposure, the $AUC_{[CSF]}/AUC_{[serum]}$ ratio was calculated for each paired injection of Bi-FC5-hFc and Bi-A20.1-mFc (Fig. 3A, insert), showing 25-fold higher apparent CNS exposure of Bi-FC5-hFc compared to Bi-A20.1-mFc.

Comparative analyses of serum (Fig. 3B, upper panel) and CSF (Fig. 3B, middle panel) levels and CSF/serum ratios (Fig. 3B, bottom panel) of Bi-FC5-hFc, Mono-FC5-hFc, and controls (Bi-A20.1-mFc and anti-HEL IgG) were performed 4 h after systemic administration of molar equivalents of molecules (6 mg/kg, 5 mg/kg, 6.25 mg/kg and 11.1 mg/kg, respectively). Although the CSF/serum ratio of Bi-FC5-hFc was slightly higher than that of Mono-FC5-hFc this difference was not statistically significant whereas both were significantly higher compared to controls (Fig. 3B, bottom panel).

Systemic pharmacological potency of V_{HH} - and V_{HH} -Fc-neuropeptide conjugates

To evaluate the transport of non-permeable molecules across the BBB, CNS centrally active analgesic peptides (Dalgargin or NPY) were covalently linked to FC5 or hFc fusion variants and evaluated for their ability to elicit pharmacological response in inflammation-induced thermal hyperalgesia. Dalgargin conjugation with Bi-FC5-hFc occasionally resulted in

15-25% reduction in P_{app} values (Fig. S1); protein conjugation batches with $P_{app} < 100 \times 10^{-6}$ cm/min were excluded from further *in vivo* studies.

Analgesic effect of FC5-Dal

Opioid peptide Dalargin (Dal) does not cross the BBB and is not analgesic after systemic dosing (30). Systemic dosing of FC5-Dal conjugate induced a significant analgesic response; 2- to 3- injections of FC5-Dal (one hour apart) were needed to achieve maximal analgesic response (Table 2). Control molecules EG2-Dal, A20.1-Dal, Dal alone, FC5 alone or physically mixed FC5+Dal produced no observable analgesic response after the same systemic dosing paradigm (Table 2). In contrast, Dal, EG2-Dal and FC5-Dal injected intracerebroventricularly (icv) showed a similar analgesic potency (Table 2). FC5 and EG2 alone were inactive when administered icv. The data suggest that only Dal chemically linked to FC5 can engage central opioid receptors after systemic administration.

Effect of PK and K_{dapp} on pharmacological potency

To understand the impact of an improved K_{dapp} and valency of receptor binding on BBB transport, the pharmacological efficacy of Bi-FC5-hFc-Dal and Mono-FC5-hFc-Dal was compared.

Bi-FC5-hFc-Dal induced a dose-dependent (0.5-6 mg/kg) inhibition of thermal hyperalgesia in the Hargreaves model after a single systemic injection (Fig. 4A). When compared to a single-dose escalation of FC5-Dal, Bi-FC5-hFc demonstrated a >60-fold increase in AUC [%MPE] of the response for the equivalent dose (Fig. 4B). Despite having similar serum half-life, Mono-FC5-hFc was 20% less potent than Bi-FC5-hFc (Fig. 4C). C-terminally fused hFc-Bi-FC5 was only marginally analgesic at the same dose of 6 mg/kg (Fig. 4C). hFc-

Dal had no systemic analgesic effect (Fig 4A), whereas it showed similar potency (%MPE 54.9 ± 2.4) to that of Bi-FC5-hFc (%MPE 43.3 ± 3.1) when injected icv.

To demonstrate that other BBB-impermeable peptides can be rendered systemically effective on CNS targets by conjugation to FC5, the non-opioid neuropeptide NPY (3.6 kDa) which acts on central Y1-5 receptors was SMCC-cross-linked to FC5 (as described for Dalargin) and evaluated in the Hargreaves pain model; FC5-NPY, in contrast to NPY, suppressed thermal hyperalgesia after systemic administration (Fig S2).

Competitive binding

To demonstrate *in vivo* competition of FC5-mediated transport, the analgesic response was evaluated in animals pre-treated with Bi-FC5-hFc to occupy the BBB transporter, followed by administration of Bi-FC5-hFc-Dal conjugate 30 min thereafter (Fig 5A, drawing). The analgesic response observed with 2.5 mg/kg of Bi-FC5-hFc-Dal (38%MPE) was significantly attenuated to 2.5%MPE in animals that received 6mg/kg 'cold' Bi-FC5-hFc (Fig. 5A).

To demonstrate *in vivo* competition on Dal-targeted central mu receptors, animals were dosed with 10 μ g of Dal icv to occupy the receptors, and were then given Bi-FC5-hFc-Dal systemically after 2 h (Fig 5B, drawing), when the analgesic response of centrally-administered Dal had diminished to baseline. When given after icv administration of Dal, the systemic analgesic effect of 6 mg/kg Bi-FC5-hFc-Dal was marginal (Fig. 5B), suggesting either a persistent occupancy or desensitization of mu receptors by centrally administered Dal.

Immunodetection of V_HH Fc fusion variants in brain sections

Immunodetection of human Fc was used to analyse the distribution of V_HH-Fc fusion variants in brain sections procured from the various experiments described above. In some experiments, Alexa680-labeled Bi-FC5-hFc was used to co-localize hFc immunofluorescence with the fluorescent label.

Representative photomicrographs of rat cortical brain sections of hFc injected animals (Fig. 6A) show the absence of hFc immunoreactivity (red) in either brain vessels (counter-stained in green) or the parenchyma (cell nuclei counter-stained in blue), while Bi-FC5-hFc-dosed animals (Fig 6B) show both vascular immunoreactivity and perinuclear punctate immunostaining in brain parenchyma (Fig. 6B; enlarged inserts). Cellular localization of observed punctate hFc-immunopositive structures was determined in animals injected with 2 mg/kg (6h) of Alexa680-labeled Bi-FC5-hFc. High-magnification micrographs in Fig. 6C-E show co-localization/overlap of Alexa680 fluorescence (blue) and hFc immunofluorescence (red), as well as their co-localization with the neuronal nucleus marker, NeuN (green).

Discussion

The BBB-carrier single domain antibody FC5 was isolated by phenotypic screening of the naive llama V_HH antibody library for BBB-permeable V_HHs in human brain endothelial cells as previously described (14, 31). V_HHs are small (15 kDa), monomeric (single) antigen-binding antibody fragments with excellent biophysical properties suitable as 'building blocks' for multifunctional molecules (32), including fusions with hFc domains and bi-specific antibodies (33, 34). In this study we demonstrate that FC5 fused with hFc in either a mono- or bivalent format enabled brain delivery of macromolecules, including neuropeptides, sufficient to engage CNS targets and to induce pharmacological responses.

The objective of FC5 protein engineering was to understand the relative contributions of its apparent affinity, valency and circulatory half-life on BBB transport characteristics using both *in vitro* assays and *in vivo* pharmacological models. An Fc domain of IgG confers prolonged circulatory half-life to monoclonal antibodies through binding, internalization and recycling in endothelial cells mediated by FcRn receptor (35). The cross species affinities of rat FcRn to rat and human IgG have been measured by Biacore™ and shown to have highly comparable K_d values, with virtually identical off rates (36). To eliminate potential ADCC through Fc-mediated effector function, FC5 was fused to an aglycosyl hFc domain (37) in either N-terminal (Bi-FC5-hFc) or C-terminal orientation (hFc-Bi-FC5). The agly hFc does not significantly impact the affinity of IgGs for FcRn (35) as confirmed by beta-phase pharmacokinetics of the tested molecules. The effect of valency/apparent affinity on BBB transport was explored by designing monovalent Mono-FC5-hFc. SV-ARBEC cell binding studies confirmed an increased K_{d,app} of bivalent Bi-FC5-hFc compared to monovalent Mono-FC5-hFc, while both fusion proteins showed similar plasma beta-phase half-lives, comparable to the half-life of a typical IgG mAb (38).

Transport rates across the *in vitro* BBB model (Bi-FC5-hFc > Mono-FC5-hFc ≥ FC5 > hFc-Bi-FC5) suggested that the increased K_{d,app} of bivalent Bi-FC5-hFc binding to SV-ARBEC resulted in an increased rate of transcytosis, and that C-terminal hFc fusion impaired BBB-crossing function of FC5. Interestingly, despite showing very weak binding to SV-ARBEC cells, both FC5 and Mono-FC5-hFc had 15-20-fold higher P_{app} values compared to molecular weight-matched control antibodies. hFc-Bi-FC5 displayed weak binding to SV-ARBEC and reduced transcytosis, suggesting that N-terminus of FC5 is important for conformational antigen binding that triggers endocytosis; this observation also indicated that cell binding assay is not fully

predictable of the antibody ability to initiate transcytosis, The data further suggest that the RMT *in vitro* can occur even at low affinity interaction of FC5 with its receptor, but is augmented by either improved practical affinity or receptor cross-linking by bivalent Bi-FC5-hFc. In contrast, a recent study (39) demonstrated that a monovalent mode of antibody binding to TfR is crucial for its escape from lysosomal degradation and subsequent transcytosis across the endothelial barrier. FC5 internalization into BEC occurs through clathrin-coated vesicles (15) and results in increased shedding of extracellular microvesicles (exosomes) from BEC, which contain both FC5 and its putative receptor, TMEM30A (40).

To establish PK/PD relationships for FC5 fusion molecules we used ‘surrogate’ measures including plasma/CSF partition ratios and pharmacological responses elicited after attaching a CNS-acting molecule that does not cross the BBB to each fusion molecule. An apparent CNS ‘exposure’, derived from the ratio of $AUC_{[CSF]}/AUC_{[serum]}$ levels over 96 h was on average 25-fold higher for Bi-FC5-hFc than for co-injected Bi-A20.1-mFc. Bi-FC5-hFc-Dal was ~60-fold more potent compared to FC5-Dal, and 25% more potent than monovalent Mono-FC5-hFc-Dal in inducing a pharmacological response, correlating with both *in vitro* P_{app} values and measured CSF levels of these FC5-enabled molecules. The results imply that a long circulation half-life conferred by hFc is the major contributor to increased CNS exposure and pharmacological efficacy of BBB-permeable antibodies, while an increase in the apparent affinity to RMT target contributes marginally to improved BBB-delivery. None of the control V_{HH} fusion molecules, or Dal alone had a systemic pharmacologic efficacy. It is conceivable that the BBB transport profile of Bi-FC5-hFc could be further improved by affinity optimization of FC5 binding to its brain endothelial antigen. The data suggest that the FC5-triggered RMT pathway is permissive for antibody-like macromolecules of at least 80 kDa. Since bivalent and monovalent hFc fusion

designs demonstrated similar BBB penetration and pharmacological potency, FC5 can likely be used as a platform to build BBB-permeable heterodimerized 'half' antibodies and more readily scalable bi- or tetra-valent fusions to therapeutic antibodies.

The measured pharmacological response with the surrogate opioid receptor agonist Dalargin linked to Bi-FC5-hFc lasted for 4h, despite a long circulation half-life and sustained elevated CSF levels of Bi-FC5-hFc for over 48 h. Dalargin-targeted mu opioid receptors (MOR) are known to undergo a short-term loss of responsiveness that occurs within minutes to several hours after an acute agonist exposure either *in vivo* or *in vitro* (41, 42). This 'acute tolerance' is the result of multiple processes that include a loss of MOR-effector coupling and desensitization due to endocytosis, which removes receptors from the surface membrane (within minutes to hours), and subsequent re-sensitization and recycling (within several hours) (42, 43). That this mechanism contributes to a short duration of the pharmacological response was confirmed by attenuation of the systemic pharmacological effect of Bi-FC5-hFc-Dal when MOR receptors were occupied/desensitized after icv administration of Dalargin. Similarly, the pharmacological response of Bi-FC5-hFc-Dal was competed out by pre-administration of 'un-labeled' Bi-FC5-hFc to engage/occupy the BBB transporter.

CSF levels of drugs are often used to extrapolate brain interstitial fluid (at target) levels (44–47). Approximately two-thirds of the CSF is produced by the choroid plexus as an ultrafiltrate with low concentrations of most blood-derived proteins and drugs (48). The blood-CSF barrier (i.e., apical tight junctions of the choroid plexus epithelium) is highly restrictive for macromolecules; the steady state serum/albumin ratio is about 0.005 and serum/IgG ratio is about 0.0027 (48, 49). No diffusional barrier exists between the interstitial space of the nervous tissue and the CSF and even large molecules can enter the interstitial space of the nervous tissue

from the CSF space (i.e., after icv injection) by diffusion; although their diffusion distances are short and concentration gradients sharp, this is often sufficient to engage receptors in the vicinity of the ventricular system in rodents (50). Approximately one-third of the CSF originates from the brain extracellular space (48); a continuous flow toward the CSF space (51–53) (CSF sink) prevents the establishment of diffusion equilibrium between the CSF space and the extracellular fluid.

The penetration of macromolecules from blood into CSF occurs largely through pore-like discontinuities in tight junctions (i.e., ultrafiltration). Ultrastructural experiments failed to demonstrate transcellular transport of IgG across choroid plexus (48). Therefore, in experiments described here, the CSF/plasma ratio of Bi-A20.1-mFc represents an internal control for blood-CSF barrier diffusion rates, while the high CSF levels of (same molecular weight) Bi-FC5-hFc likely originate from the brain interstitial fluid (ISF). This is further suggested by the ‘mismatched’ CSF/serum levels, with a delayed Bi-FC5-hFc CSF concentration peak occurring at 24h. The timing of the maximal PD response with FC5-enabled molecules (~1 h after systemic administration), when their CSF levels were similar to those of the ineffective A20.1-fusion molecules is another strong piece of evidence of the BBB penetration rather than CP secretion.

In addition to BBB transcytosis, an important additional ‘barrier’ to distribution of therapeutic antibodies within CNS is their limited diffusion in the brain extracellular space, restricted by its tortuosity and by binding to the extracellular matrix heparin sulfate proteoglycans (54). Due to the highly limited diffusion distances of macromolecules in the neuropil, the elimination of free antibody from brain ISF into CSF likely occurs via bulk flow; one of the hallmarks of bulk flow, compared to simple diffusion, is the independence of solute movement from molecular size (54). Estimated ISF drainage rates for albumin ($\mu\text{l} \times \text{g brain}^{-1} \times$

min⁻¹) were 0.18, 0.19, and 0.29 for the caudate nucleus, internal capsule, and midbrain respectively; the flow of ISF into bulk CSF sampled from the cisterna magna accounted for 60-75% of efflux from midbrain but only 10-15% of efflux from caudate nucleus or internal capsule (51, 55). Based on these considerations, the measured CSF levels of Bi-FC5-hFc are likely an underestimation of its ISF levels. Since direct measurement of ISF unbound levels of therapeutic antibodies by microdialysis is not feasible due to their size (56), we used in situ detection by immunofluorescence to demonstrate the presence of Bi-FC5-hFc in the neuropil, co-localizing with vascular and neuronal markers.

The extensive literature (7, 8, 39, 57) on TfR and IR antibodies reports a range of their serum/brain partitions (from 0.1-4 %ID/g vs. 0.002 %ID/g for IgG), often significantly influenced by the affinity and valency of binding to the RMT receptor (8, 39, 57). The direct comparison of their BBB delivery capacity with engineered FC5 variants remains difficult due to the lack of side-by-side studies using the same experimental designs and analytical methods. A ubiquitous distribution and physiological importance of TfR and IR carries safety risks as recently reported, including complement-mediated lysis of TfR-rich reticulocytes (13), and pancreatic toxicity of the IR antibody-GDNF fusion protein in non-human primates (12). This underscores the need for alternative RMT carriers that can be engineered and developed as a platform to enhance CNS delivery. Species cross-reactivity and modularity of potential designs offered by FC5 as the BBB-carrier arm could enable translational modeling and eventually the development of BBB-permeable therapeutics for the treatment of CNS diseases.

Acknowledgments:

We thank Luc Tessier, NRC for maintenance of nanoLC-SRM instruments and Ellen Rohde, BiogenIdec for running and analyzing pharmacokinetics of various molecules in the rat, Chioma Nwankwo, You Li and Nels Pederson for cloning of various molecules, Jorge Sanchez-Salazar and Tom Cameron for cell line development and expression, and Monika Vecchi, Susan Foley, YuTing Huang, Yaping Sun, Dingyi Wen for review of mass spectrometry analysis.

The study was funded through program support from Biogen Idec Corporation based on yearly program reviews and prioritization, and through National Research Council of Canada support for the strategic program Therapeutics beyond Brain Barriers.

References:

1. Abbott, N. J., Patabendige, A. A. K., Dolman, D. E. M., Yusof, S. R., and Begley, D. J. (2010) Structure and function of the blood-brain barrier. *Neurobiol Dis* **37**, 13–25
2. Stanimirovic, D. B., and Friedman, A. (2012) Pathophysiology of the neurovascular unit: disease cause or consequence? *J Cereb Blood Flow Metab* **32**, 1207–21
3. Hartz, A. M. S., and Bauer, B. (2011) ABC transporters in the CNS - an inventory. *Curr Pharm Biotechnol* **12**, 656–73
4. Pardridge, W. M. (2002) Drug and gene delivery to the brain: the vascular route. *Neuron* **36**, 555–8
5. Jones, A. R., and Shusta, E. V (2007) Blood-brain barrier transport of therapeutics via receptor-mediation. *Pharm Res* **24**, 1759–71
6. Xiao, G., and Gan, L.-S. (2013) Receptor-mediated endocytosis and brain delivery of therapeutic biologics. *Int J Cell Biol* **2013**, 703545
7. Pardridge, W. M., Buciak, J. L., and Friden, P. M. (1991) Selective transport of an anti-transferrin receptor antibody through the blood-brain barrier in vivo. *J Pharmacol Exp Ther* **259**, 66–70
8. Coloma, M. J., Lee, H. J., Kurihara, A., Landaw, E. M., Boado, R. J., Morrison, S. L., and Pardridge, W. M. (2000) Transport across the primate blood-brain barrier of a genetically engineered chimeric monoclonal antibody to the human insulin receptor. *Pharm Res* **17**, 266–74
9. Demeule, M., Currie, J.-C., Bertrand, Y., Ché, C., Nguyen, T., Régina, A., Gabathuler, R., Castaigne, J.-P., and Béliveau, R. (2008) Involvement of the low-density lipoprotein receptor-related protein in the transcytosis of the brain delivery vector angiopep-2. *J Neurochem* **106**, 1534–44
10. Boado, R. J., Lu, J. Z., Hui, E. K.-W., Sumbria, R. K., and Pardridge, W. M. (2013) Pharmacokinetics and brain uptake in the rhesus monkey of a fusion protein of arylsulfatase a and a monoclonal antibody against the human insulin receptor. *Biotechnol Bioeng* **110**, 1456–65
11. Boado, R. J., and Pardridge, W. M. (2009) Comparison of blood-brain barrier transport of glial-derived neurotrophic factor (GDNF) and an IgG-GDNF fusion protein in the rhesus monkey. *Drug Metab Dispos* **37**, 2299–304
12. Ohshima-Hosoyama, S., Simmons, H. A., Goecks, N., Joers, V., Swanson, C. R., Bondarenko, V., Velotta, R., Brunner, K., Wood, L. D., Hruban, R. H., and Emborg, M. E.

(2012) A monoclonal antibody-GDNF fusion protein is not neuroprotective and is associated with proliferative pancreatic lesions in parkinsonian monkeys. *PLoS One* **7**, e39036

13. Couch, J. A., Yu, Y. J., Zhang, Y., Tarrant, J. M., Fuji, R. N., Meilandt, W. J., Solanoy, H., Tong, R. K., Hoyte, K., Luk, W., Lu, Y., Gadkar, K., Prabhu, S., Ordonia, B. A., Nguyen, Q., Lin, Y., Lin, Z., Balazs, M., Scarce-Levie, K., Ernst, J. A., Dennis, M. S., and Watts, R. J. (2013) Addressing safety liabilities of TfR bispecific antibodies that cross the blood-brain barrier. *Sci Transl Med* **5**, 183ra57, 1–12
14. Muruganandam, A., Tanha, J., Narang, S., and Stanimirovic, D. (2002) Selection of phage-displayed llama single-domain antibodies that transigrate across human blood-brain barrier endothelium. *FASEB J* **16**, 240–2
15. Abulrob, A., Sprong, H., Van Bergen en Henegouwen, P., and Stanimirovic, D. (2005) The blood-brain barrier transigrating single domain antibody: mechanisms of transport and antigenic epitopes in human brain endothelial cells. *J Neurochem* **95**, 1201–14
16. Haqqani, A. S., Caram-Salas, N., Ding, W., Brunette, E., Delaney, C. E., Baumann, E., Boileau, E., and Stanimirovic, D. (2013) Multiplexed evaluation of serum and CSF pharmacokinetics of brain-targeting single-domain antibodies using a NanoLC-SRM-ILIS method. *Mol Pharm* **10**, 1542–56
17. Iqbal, U., Trojahn, U., Albaghdadi, H., Zhang, J., O'Connor-McCourt, M., Stanimirovic, D., Tomanek, B., Sutherland, G., and Abulrob, A. (2010) Kinetic analysis of novel mono- and multivalent VHH-fragments and their application for molecular imaging of brain tumours. *Br J Pharmacol* **160**, 1016–28
18. Tanha, J., Dubuc, G., HIRAMA, T., Narang, S. A., and MacKenzie, C. R. (2002) Selection by phage display of llama conventional V(H) fragments with heavy chain antibody V(H)H properties. *J Immunol Methods* **263**, 97–109
19. Farrington, G. K., Saeed-Kothe, A., Garber, E., and Lugovskoy, A. A. (2009) Single-chain Fc (scFc) regions, binding polypeptides comprising same, and methods related thereto. US 20090252729 A1 patent.
20. Mattson, G., Conklin, E., Desai, S., Nielander, G., Savage, M. D., and Morgensen, S. (1993) A practical approach to crosslinking. *Mol Biol Rep* **17**, 167–83
21. Haqqani, A. S., Kelly, J. F., and Stanimirovic, D. B. (2008) Quantitative protein profiling by mass spectrometry using label-free proteomics. *Methods Mol Biol* **439**, 241–56
22. Lin, D., Alborn, W. E., Slebos, R. J. C., and Liebler, D. C. (2013) Comparison of protein immunoprecipitation-multiple reaction monitoring with ELISA for assay of biomarker candidates in plasma. *J Proteome Res* **12**, 5996–6003

23. Garberg, P., Ball, M., Borg, N., Cecchelli, R., Fenart, L., Hurst, R. D., Lindmark, T., Mabondzo, A., Nilsson, J. E., Raub, T. J., Stanimirovic, D., Terasaki, T., Oberg, J.-O., and Osterberg, T. (2005) In vitro models for the blood-brain barrier. *Toxicol Vitro* **19**, 299–334
24. Artursson, P., and Karlsson, J. (1991) Correlation between oral drug absorption in humans and apparent drug permeability coefficients in human intestinal epithelial (Caco-2) cells. *Biochem Biophys Res Commun* **175**, 880–5
25. Kornhuber, M. E., Kornhuber, J., and Cimniak, U. (1986) A method for repeated CSF sampling in the freely moving rat. *J Neurosci Methods* **17**, 63–8
26. Sarna, G., Hutson, P. H., and Curzon, G. (1984) A technique for repeated sampling of cerebrospinal fluid in freely moving rats and its uses. *J Physiol (Paris)* **79**, 536–7
27. Nirogi, R., Kandikere, V., Mudigonda, K., Bhyrapuneni, G., Muddana, N., Saralaya, R., and Benade, V. (2009) A simple and rapid method to collect the cerebrospinal fluid of rats and its application for the assessment of drug penetration into the central nervous system. *J Neurosci Methods* **178**, 116–9
28. Fluttert, M., Dalm, S., and Oitzl, M. S. (2000) A refined method for sequential blood sampling by tail incision in rats. *Lab Anim* **34**, 372–8
29. Paxinos, G., Watson, C., Pennisi, M., and Topple, A. (1985) Bregma, lambda and the interaural midpoint in stereotaxic surgery with rats of different sex, strain and weight. *J Neurosci Methods* **13**, 139–43
30. Rousselle, C., Clair, P., Smirnova, M., Kolesnikov, Y., Pasternak, G. W., Gac-Breton, S., Rees, A. R., Scherrmann, J.-M., and Tamsamani, J. (2003) Improved brain uptake and pharmacological activity of dalargin using a peptide-vector-mediated strategy. *J Pharmacol Exp Ther* **306**, 371–6
31. Tanha, J., Muruganandam, A., and Stanimirovic, D. (2003) Phage display technology for identifying specific antigens on brain endothelial cells. *Methods Mol Med* **89**, 435–49
32. Muyldermans, S. (2013) Nanobodies: natural single-domain antibodies. *Annu Rev Biochem* **82**, 775–97
33. Van Bockstaele, F., Holz, J.-B., and Revets, H. (2009) The development of nanobodies for therapeutic applications. *Curr Opin Investig drugs* **10**, 1212–24
34. Vincke, C., and Muyldermans, S. (2012) Introduction to heavy chain antibodies and derived Nanobodies. *Methods Mol Biol* **911**, 15–26
35. Giragossian, C., Clark, T., Piché-Nicholas, N., and Bowman, C. J. (2013) Neonatal Fc receptor and its role in the absorption, distribution, metabolism and excretion of immunoglobulin G-based biotherapeutics. *Curr Drug Metab* **14**, 764–90

36. Vaughn, D. E., and Bjorkman, P. J. (1997) High-affinity binding of the neonatal Fc receptor to its IgG ligand requires receptor immobilization. *Biochemistry* **36**, 9374–80
37. Hristodorov, D., Fischer, R., and Linden, L. (2013) With or without sugar? (A)glycosylation of therapeutic antibodies. *Mol Biotechnol* **54**, 1056–68
38. Dirks, N. L., and Meibohm, B. (2010) Population pharmacokinetics of therapeutic monoclonal antibodies. *Clin Pharmacokinet* **49**, 633–59
39. Niewoehner, J., Bohrmann, B., Collin, L., Urich, E., Sade, H., Maier, P., Rueger, P., Stracke, J. O., Lau, W., Tissot, A. C., Loetscher, H., Ghosh, A., and Freskgård, P.-O. (2014) Increased brain penetration and potency of a therapeutic antibody using a monovalent molecular shuttle. *Neuron* **81**, 49–60
40. Haqqani, A. S., Delaney, C. E., Tremblay, T.-L., Sodja, C., Sandhu, J. K., and Stanimirovic, D. B. (2013) Method for isolation and molecular characterization of extracellular microvesicles released from brain endothelial cells. *Fluids Barriers CNS* **10**, 4
41. Dang, V. C., Napier, I. A., and Christie, M. J. (2009) Two distinct mechanisms mediate acute mu-opioid receptor desensitization in native neurons. *J Neurosci* **29**, 3322–7
42. Dang, V. C., and Christie, M. J. (2012) Mechanisms of rapid opioid receptor desensitization, resensitization and tolerance in brain neurons. *Br J Pharmacol* **165**, 1704–16
43. Williams, J. T., Ingram, S. L., Henderson, G., Chavkin, C., von Zastrow, M., Schulz, S., Koch, T., Evans, C. J., and Christie, M. J. (2013) Regulation of μ -opioid receptors: desensitization, phosphorylation, internalization, and tolerance. *Pharmacol Rev* **65**, 223–54
44. De Lange, E. C. M., and Danhof, M. (2002) Considerations in the use of cerebrospinal fluid pharmacokinetics to predict brain target concentrations in the clinical setting: implications of the barriers between blood and brain. *Clin Pharmacokinet* **41**, 691–703
45. Shen, D. D., Artru, A. A., and Adkison, K. K. (2004) Principles and applicability of CSF sampling for the assessment of CNS drug delivery and pharmacodynamics. *Adv Drug Deliv Rev* **56**, 1825–57
46. Lin, J. H. (2008) CSF as a surrogate for assessing CNS exposure: an industrial perspective. *Curr Drug Metab* **9**, 46–59
47. Pepinsky, R. B., Shao, Z., Ji, B., Wang, Q., Meng, G., Walus, L., Lee, X., Hu, Y., Graff, C., Garber, E., Meier, W., and Mi, S. (2011) Exposure levels of anti-LINGO-1 Li81 antibody in the central nervous system and dose-efficacy relationships in rat spinal cord remyelination models after systemic administration. *J Pharmacol Exp Ther* **339**, 519–29

48. Johanson, C. E., Stopa, E. G., and McMillan, P. N. (2011) The blood-cerebrospinal fluid barrier: structure and functional significance. *Methods Mol Biol* **686**, 101–31
49. Strazielle, N., and Gherzi-Egea, J. F. (2013) Physiology of blood-brain interfaces in relation to brain disposition of small compounds and macromolecules. *Mol Pharm* **10**, 1473–91
50. Yan, Q., Matheson, C., Sun, J., Radeke, M. J., Feinstein, S. C., and Miller, J. A. (1994) Distribution of intracerebral ventricularly administered neurotrophins in rat brain and its correlation with trk receptor expression. *Exp Neurol* **127**, 23–36
51. Szentistványi, I., Patlak, C. S., Ellis, R. A., and Cserr, H. F. (1984) Drainage of interstitial fluid from different regions of rat brain. *Am J Physiol* **246**, F835–44
52. Abbott, N. J. (2004) Evidence for bulk flow of brain interstitial fluid: significance for physiology and pathology. *Neurochem Int* **45**, 545–52
53. Iliff, J. J., Wang, M., Liao, Y., Plogg, B. A., Peng, W., Gundersen, G. A., Benveniste, H., Vates, G. E., Deane, R., Goldman, S. A., Nagelhus, E. A., and Nedergaard, M. (2012) A paravascular pathway facilitates CSF flow through the brain parenchyma and the clearance of interstitial solutes, including amyloid β . *Sci Transl Med* **4**, 147ra111
54. Wolak, D. J., and Thorne, R. G. (2013) Diffusion of macromolecules in the brain: implications for drug delivery. *Mol Pharm* **10**, 1492–504
55. Cserr, H. F., Cooper, D. N., Suri, P. K., and Patlak, C. S. (1981) Efflux of radiolabeled polyethylene glycols and albumin from rat brain. *Am J Physiol* **240**, F319–28
56. Caljon, G., Caveliers, V., Lahoutte, T., Stijlemans, B., Ghassabeh, G. H., Van Den Abbeele, J., Smolders, I., De Baetselier, P., Michotte, Y., Muyldermans, S., Magez, S., and Clinckers, R. (2012) Using microdialysis to analyse the passage of monovalent nanobodies through the blood-brain barrier. *Br J Pharmacol* **165**, 2341–53
57. Yu, Y. J., Zhang, Y., Kenrick, M., Hoyte, K., Luk, W., Lu, Y., Atwal, J., Elliott, J. M., Prabhu, S., Watts, R. J., and Dennis, M. S. (2011) Boosting brain uptake of a therapeutic antibody by reducing its affinity for a transcytosis target. *Sci Transl Med* **3**, 84ra44
58. Hussack, G., Arbabi-Ghahroudi, M., van Faassen, H., Songer, J. G., Ng, K. K.-S., MacKenzie, R., and Tanha, J. (2011) Neutralization of *Clostridium difficile* toxin A with single-domain antibodies targeting the cell receptor binding domain. *J Biol Chem* **286**, 8961–76
59. Iqbal, U., Abulrob, A., and Stanimirovic, D. B. (2011) Integrated platform for brain imaging and drug delivery across the blood-brain barrier. *Methods Mol Biol* **686**, 465–81

Table 1. V_HHs and Fc domains used in the study for engineering V_HH-Fc fusions and peptides used in their nanoLC-SRM detection.

Protein	Refs	Type	MW (kDa)	Pep No	Peptide Sequence	Charge	m/z of peptide	Peptide fragment signatures (m/z) used for quantification	LOQ (pM) ^(c)
FC5	(14, 15)	V _H H, llama naive	15.3	1	ITWGGDNTFYNSVK	2	844.92	534.48, 729.47, 737.89, 1288.44	25
					ITWGGDNTFYNSVK ^(b)	2	848.92	542.48, 733.48, 741.87, 1296.44	25
A20.1	(58)	V _H H, llama immune (C. diff toxin)	16.8	2	TFSMDPMAWFR	2	694.77	582.22, 807.4, 922.42, 1140.5	33
				3	TTYADSVK	2	524.23	203.1, 682.34, 845.4	66
				4	EFVAAGSSTGR	2	541.29	500.12, 564.32, 635.28, 706.44	50
				5	DEYAYWGQGTQTVSSGQAGQ GSEQK	2	1381.47	1061.0, 1163.5, 1580.4, 1598.5, 1748.8	50
EG2	(59)	V _H H, llama immune (EGFR)	15.9	6	DFSDYVMGWFR	2	711.72	322.31, 565.31, 696.43, 795.42, 858.18, 1101.29, 1160.49	25
				7	NMVYLQMNSLKPEDTAVYYCA VNSAGTYVSPR	3	1215.57	359.09, 621.29, 779.49, 1432.47, 1511.95, 1633.58, 1642.91, 1689.09	66
hFc	(37)	Human agly Fc domain		8	TTPPVLDSDGSFFLYSK	2	937.28	836.8, 1150.24, 1265.44, 1378.72, 1477.44	8
					TTPPVLDSDGSFFLYSK ^(b)	2	941.28	840.5, 1158.25, 1273.44, 1386.74, 1485.44	8
				9	GTQVTVSSAEPK	2	602.27	818.25, 831.28, 960.32	100
				10	TPEVTCVVVDVSHEDPEVK	3	713.65	472.33, 834.5, 971.5	25
mFc		Mouse Fc domain		11	APQVYILPPPAEQLSR	2	889.84	672.5, 785.42, 994.58	33
				12	TDSFSCNVR	2	543.23	635.42, 782.5, 869.58	33
Anti- HEL		Mouse IgG1 m297Q	148.6	13	EVQLEQSGAELMKPGASVK	2	1001.49	558.46, 686.58, 930.57, 1187.68	17
					EVQLEQSGAELMKPGASVK ^(b)	2	1005.49	566.46, 694.58, 938.57, 1195.68	17
Albumin ^(a)			66	14	NTEPVLDSDGSYFMYSK	2	976.54	804.83, 1184.7, 1299.5, 1412.33, 1608.5	66
				15	DNCFATEGPNLVAR	2	782.32	246.16, 346.28, 1174.48	-
				16	APQVSTPTLVEAAR	2	720.84	703.0, 856.9, 957.9, 1044.8, 1143.7	-

- (a) In various studies, assays were multiplexed in different combinations for simultaneous monitoring in the same sample (e.g., FC5+A20.1+ albumin; Bi-FC5-hFc + Bi-A20.1-mFc etc.). The location of peptide chosen in relation to CDRs of each antibody is shown in Supplementary Figure S1.
- (b) Isotopically labeled internal standards (ILIS)
- (c) Limits of quantitation (LOQ) is shown in picomoles per litres (pM). LOQ of each peptide was determined from a dilution series (50-2000 attomole) of each protein digest or ILIS peptide analyzed by nanoLC-SRM.

Table 2. Summary of thermal hyperalgesia suppression in the Hargreaves model using Dalargin alone or linked to FC5 or control VHHs, EG2 and A20.1. The data are expressed as the percentage of maximum possible effect [%MPE \pm SD for 3-6 animals] calculated from the areas under the response curves for contralateral paw (maximal effect) and inflamed paw over the duration of the response (4h). Iv dose (in mg/kg) was repeated three times (one hour apart; time 0 h, 1 h and 2 h).

molecule	ICV		IV	
	Dose (μ g)	% MPE	Dose (mg/kg) x 3 injections	% MPE
PBS	5 μ l	0 \pm 0.8	800 μ l	0.1 \pm 0.6
Dalargin	2	35 \pm 1 ^{*,#}	0.34	0.3 \pm 0.3
FC5	70	0.1 \pm 2	7.0	1.9 \pm 0.3
EG2	70	0.1 \pm 2	7.0	0.2 \pm 1.3
A20.1			7.8	2.2 \pm 0.3
FC5-Dalargin	75	45 \pm 3 [*]	7.0	41 \pm 0.5 [*]
EG2-Dalargin	75	31 \pm 1 ^{*,#}	7.0	2.0 \pm 0
A20.1-Dalargin			2.5	3.1 \pm 0
FC5 + Dalargin			0.65 + 7.0	0 \pm 1.6

Figure legends:

Fig. 1. Design, biophysical characteristics of FC5 fusions with human Fc. A) A structural representation of each molecule is shown (left to right) FC5, Bi-FC5-hFc, Mono-FC5-hFc and hFc-Bi-FC5 (d). B) Coomassie brilliant blue stained reducing and non-reducing SDS 4-20% gradient PAGE of final purified pools of antibodies. Standards are in lane 1 (molecular weights in kDa are as indicated to the left of the gel).

Fig 2. Cell binding and *in vitro* BBB transport of FC5 fusions with human Fc. A) FACS binding curves to SV-ARBEC of Bi-FC5-hFc, Mono-FC5-hFc and hFc-Bi-FC5. The curve was fitted as described in the Materials and Methods section. K_{dapp} derived for Bi-FC5-hFc was 46 ± 5 nM. hFc-Bi-FC5 and Mono-FC5-hFc did not reach saturation in the FACS assay therefore these data were not curve fitted. B) P_{app} values for monovalent antibodies, FC5, Bi-FC5-hFc, Mono-FC5-hFc and hFc-Bi-FC5 paired with corresponding controls (V_{HH} EG2 or IgG anti-Hel) co-applied in the same Transwell insert. *In vitro* BBB transport studies and P_{app} calculations were performed as described in Materials and Methods. The levels of antibodies in the bottom chamber (15, 30, 60 and 90 min) were determined by SRM-ILIS as described. Values are Means \pm SD of P_{app} values derived from 5-10 separate Transwell inserts. Asterisks on bars represent statistically significant difference as determined by ANOVA Bonferroni post hoc test, where FC5 and Mono-FC5-hFc showed $p < 0.05$ (*) and Bi-FC5-hFc showed $p < 0.01$ (**). compared to controls.

Fig 3. Serum and CSF pharmacokinetics of FC5hFc. A) Bi-FC5-hFc and Bi-A20.1-mFc were co-administered via the tail vein at 6 mg/kg each, and antibody levels at indicated time points

after injection were determined in blood (upper panel) and CSF (middle panel) samples from the cisterna magna. Paired CSF/serum ratio (%) at each time point are plotted in lower panel. The insert shows percentage CNS exposure calculated as a ratio of AUC_{CSF}/AUC_{serum} from each paired antibody administration. Results are shown as Means \pm SD from 4 separate animals. CSF levels and the CSF/serum ratio of Bi-FC5-hFc were significantly higher ($p < 0.01$; two-way ANOVA) from paired Bi-A20.1-mFc levels at each time point after systemic injection. **B)** Serum (upper panel) and CSF (middle panel) levels and CSF/serum ratios (lower panel) of Bi-FC5-hFc (6 mg/kg), Mono-FC5-hFc (5 mg/kg), Anti-HEL IgG (11.1 mg/kg) or Bi-A20.1-mFc (6.25 mg/kg) 4 h after systemic administration. Results are shown as Means \pm SD from 3-6 separate animals. Asterisks on bars represent statistically significant difference as determined by ANOVA Bonferroni post hoc test, where both Bi-FC5-hFc and Mono-FC5-hFc showed $p < 0.05$ (*) compared to control antibodies Anti-HEL IgG and Bi-A20.1-mFc. Serum and CSF levels of antibodies were determined by SRM-ILIS method as described in Materials and Methods.

Fig 4. Effects of FC5 fusions with human Fc cross-linked with Dalargin on thermal hyperalgesia in Hargreaves model of inflammatory pain. **A)** Latency of withdrawal of control intact paw (open squares) or inflamed paw to a thermal stimulus was measured after a single iv dose 0.5 mg/kg (closed circles), 2.5 mg/kg (open circles) or 6 mg/kg (closed squares) Bi-FC5-hFc-Dal, 6mg/kg (closed triangles) hFc-Dal or PBS in 15 min intervals over 4 h. Data are shown as means \pm SD for 3-4 separate animals in each group. **B)** Analgesic effect achieved with a single iv. injection of escalating doses of FC5-Dal or Bi-FC5-hFc-Dal. Data are the integrated AUC over the duration of response (4h) expressed as percent MPE (control paw) (mean \pm SD of 3-6 animals in each group). **C)** Analgesic response achieved with a single, 6

mg/kg dose of hFc-Dal, Mono-FC5-hFc-Dal, Bi-FC5-hFc-Dal or hFc-Bi-FC5-Dal. The data are integrated AUC expressed as percent MPE (control paw) (means \pm SD of at 3-6 animals in each group). The experiments in B) and C) were performed with different conjugation 'batches' of molecules in different sets of animals.

Fig 5. Competition of BBB transporter and MOR receptors. A) The effect of administration of 'cold' Bi-FC5-hFc on systemic analgesic effect of subsequent Bi-FC5-hFc-Dal in the Hargreaves inflammatory hyperalgesia model. Animals were given 2.5 mg/kg Bi-FC5-hFc-Dal (open circles) or 6 mg/kg Bi-FC5-hFc 1 h prior to 2.5 mg/kg Bi-FC5-hFc-Dal. B) The effect of icv administration of Dalargin on systemic analgesic effect of Bi-FC5-hFc-Dal in the Hargreaves inflammatory hyperalgesia model. Animals received 10 μ g Dalargin icv (open circles) and analgesic effect was followed over 2 h until it diminished to basal levels; animals then received one iv dose of 6 mg/kg Bi-FC5-hFc-Dal (closed circles) and the analgesic effect was measured over the ensuing 2 h. Left panels in A and B show a pictorial rendering of experimental design; middle panels show latency of withdrawal of inflamed or control paw (open squares) to a thermal stimulus in the Hargreaves model. Right panels show the integrated AUC expressed as percent MPE (control paw). Data are means \pm SD of at 4-6 animals in each group. The (*) indicates a significant difference ($p < 0.01$; ANOVA) between Bi-FC5-hFc-Dal response with and without competing molecules.

Fig 6. Immunodetection of Bi-FC5-hFc in brain sections. Panels A-B are fluorescence micrographs of brain sections (frontal cortex) collected 24 h after 6 mg/kg iv dose of either hFc (A) or Bi-FC5-hFc (B and B'), immunostained with anti-human Fc antibody (red) and

counterstained with the vessel-binding Tomato lectin (green) and Hoechst to visualize cell nuclei (blue). Panels C-E are fluorescence micrographs of brain sections (cortex) derived 6 h after 2 mg/kg iv dose of Bi-FC5-hFc conjugated with the fluorescent dye Al680 (blue), and immunostained with anti-hFc antibody (red) and antibody specific to neuronal antigen, NeuN (green).

Supplementary figure legends:

Fig S1. Effect of Dalargin cross-linking on P_{app} values of Bi-FC5-hFc. Two batches (1) and (2) of Bi-FC5-hFc-Dalargin conjugate show a 50% and 30% reduction in P_{app} values, respectively, compared to unconjugated Bi-FC5-hFc. Anti-HEL IgG was used as the internal control in each insert. Each point represents a P_{app} value derived from a separate insert. Bi-FC5-hFc-Dal conjugates showing P_{app} range of 150-200 cm/min were used in subsequent *in vivo* studies.

Fig S2. Effects of neuropeptide Y (NPY) chemically conjugated to FC5 on thermal hyperalgesia in Hargreaves model of inflammatory pain. A) Latency of withdrawal of control intact paw (open squares) or inflamed paw to a thermal stimulus was measured after two doses of PBS (500 μ l each) (open triangles) or NPY (2.02 mg/kg each) (open circles) or FC5-NPY (6.6 mg/kg each) (closed circles) given one hour apart (time 0 and 1 h). Data are shown as means \pm SD for 3-4 separate animals in each group. B) Analgesic effect achieved after either iv or icv administration of PBS, NPY and FC5-NPY shown as the integrated AUC over the duration of

response (4h) expressed as percent MPE (control paw) (mean \pm SD of 3-6 animals in each group). For central effect, the rats received one icv injection of 2.5 μ g NPY or 93 μ g FC5-NPY.

* - indicates statistical difference ($p < 0.01$; ANOVA) from NPY.

Fig S3. Location of SRM signatures used for quantitative analyses of various VHHs and human and mouse Fc.

Table S1. In-line light scattering analysis and evaluation of average number of Dalargin peptides linked to each molecule. The number of conjugated Dalargin molecules was determined by MS from peaks eluting from gel filtration studies.

Molecule plasmid	FC5 ⁽¹⁾ (EAG2333)	Bi-FC5-hFc ⁽²⁾ (EAG2345)	Mono-FC5-hFc ⁽²⁾ (EAG2304)	hFc
Calculated Mwt (Daltons)	15,375	78,480	66,395	51,896
LS Mwt (Daltons)	15,980	77,530	78,950	57,800
Avg linked Dalargin peptides ⁽³⁾	1.5	1.5	1.5	1.0

(1) contains myc tag EQKLISEEDL, C-termini (1202 mwt), C-terminal His tag 5H

(2) Fc domains are human IgG1 and agly (all Fc domains contain a T299A point mutation in the hIgG sequence to eliminate Fc N-glycosylation)

(3) evaluated by MS, to determine the average number of Dalargin molecules covalently linked to the FC5-hFc domains.

Figure 1.

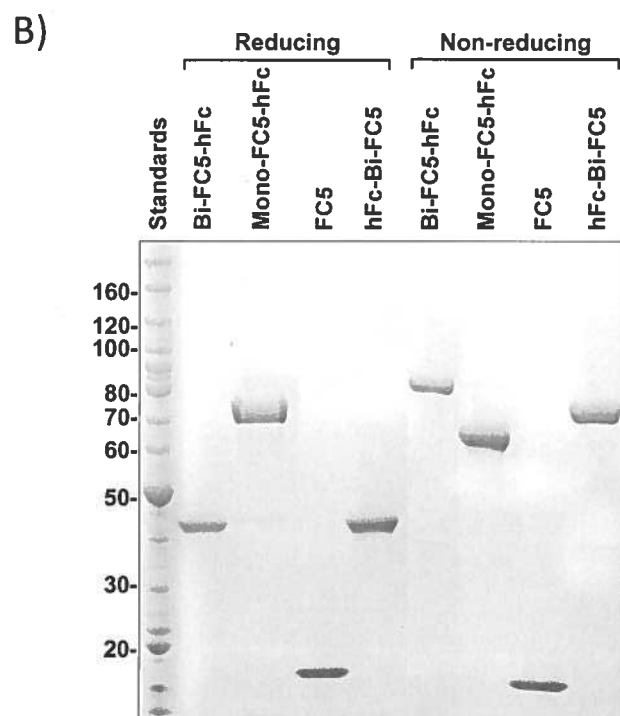
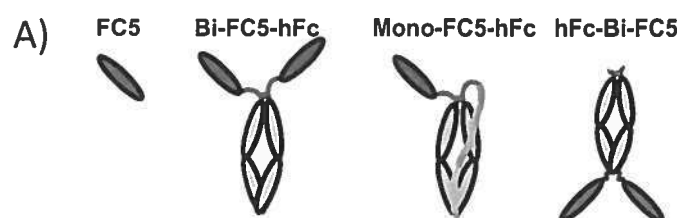


Figure 2.

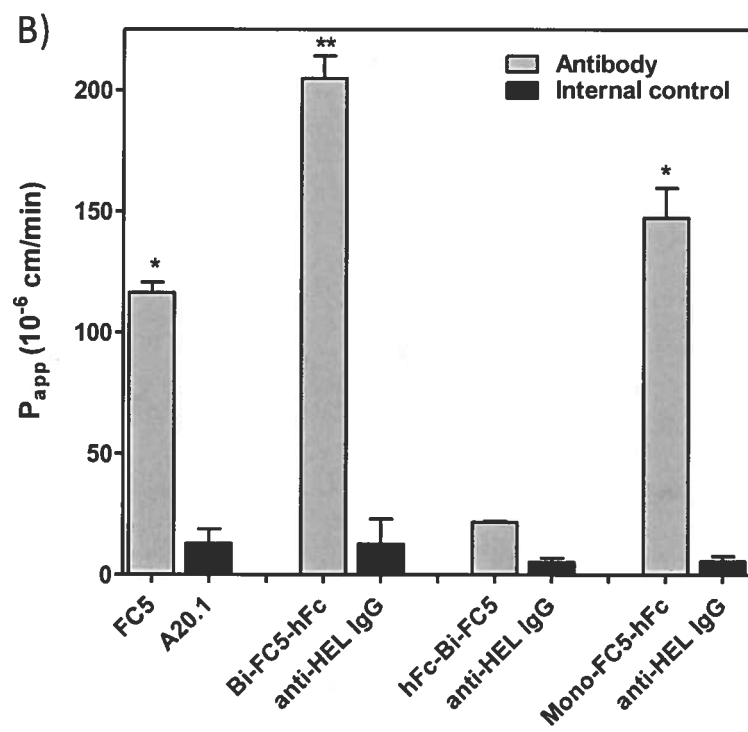
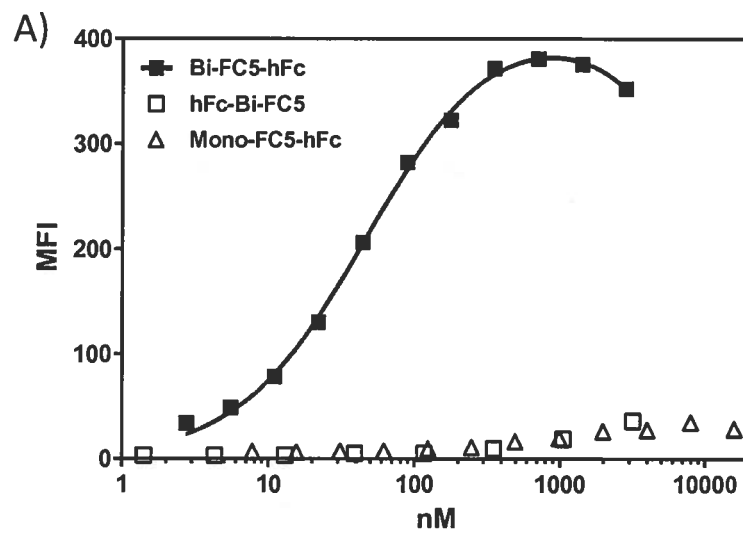


Figure 3.

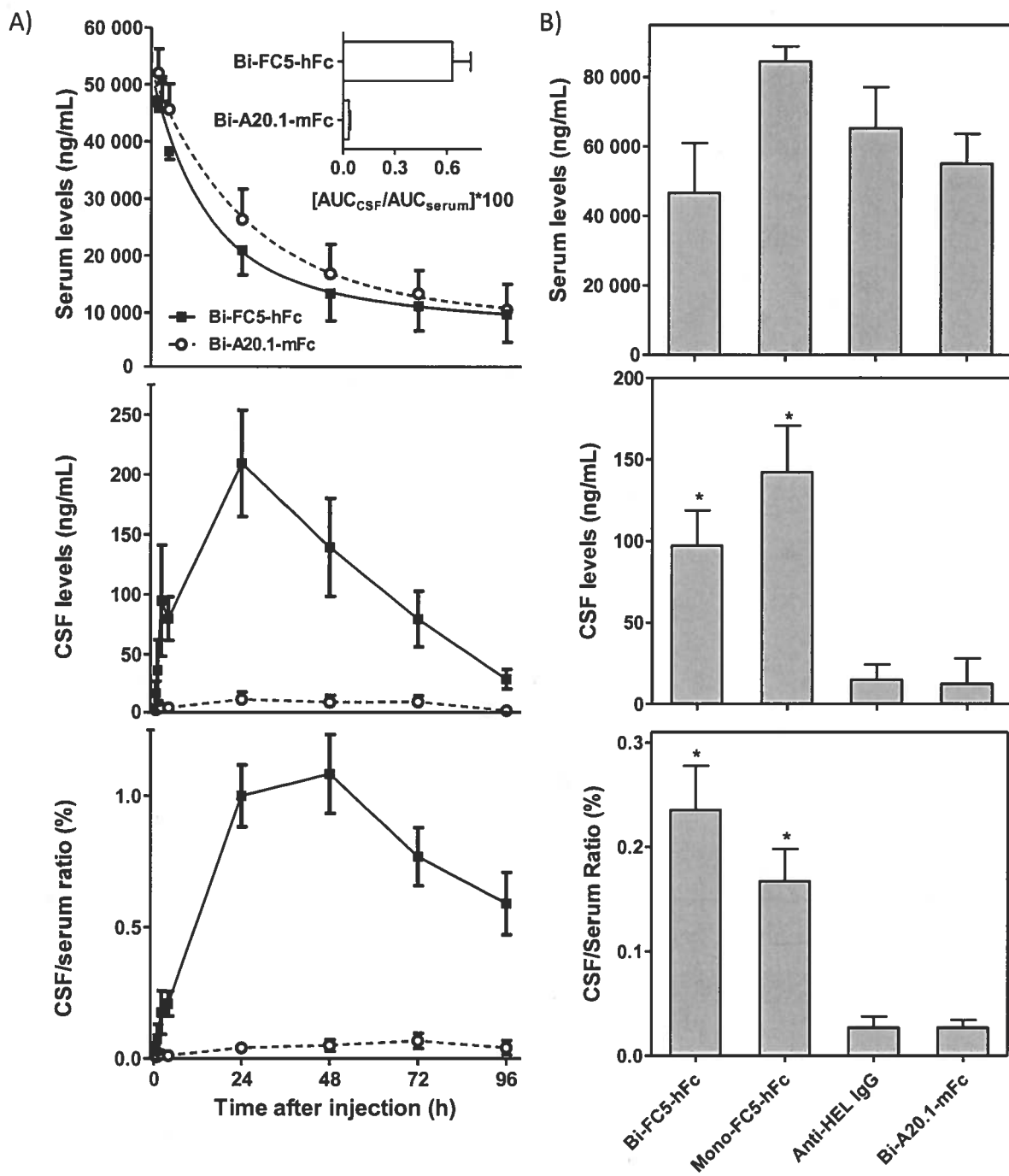


Figure 4.

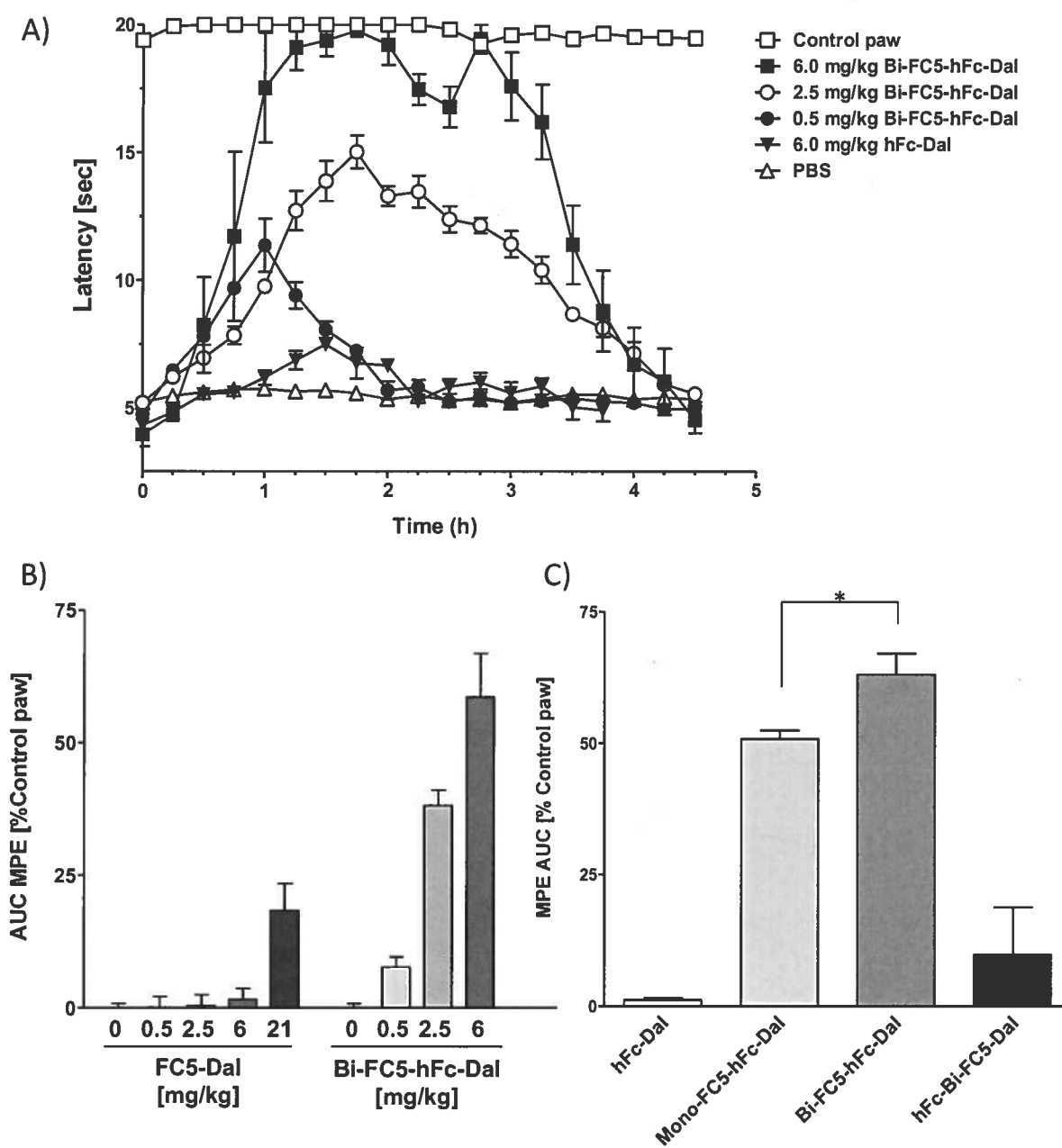


Figure 5.

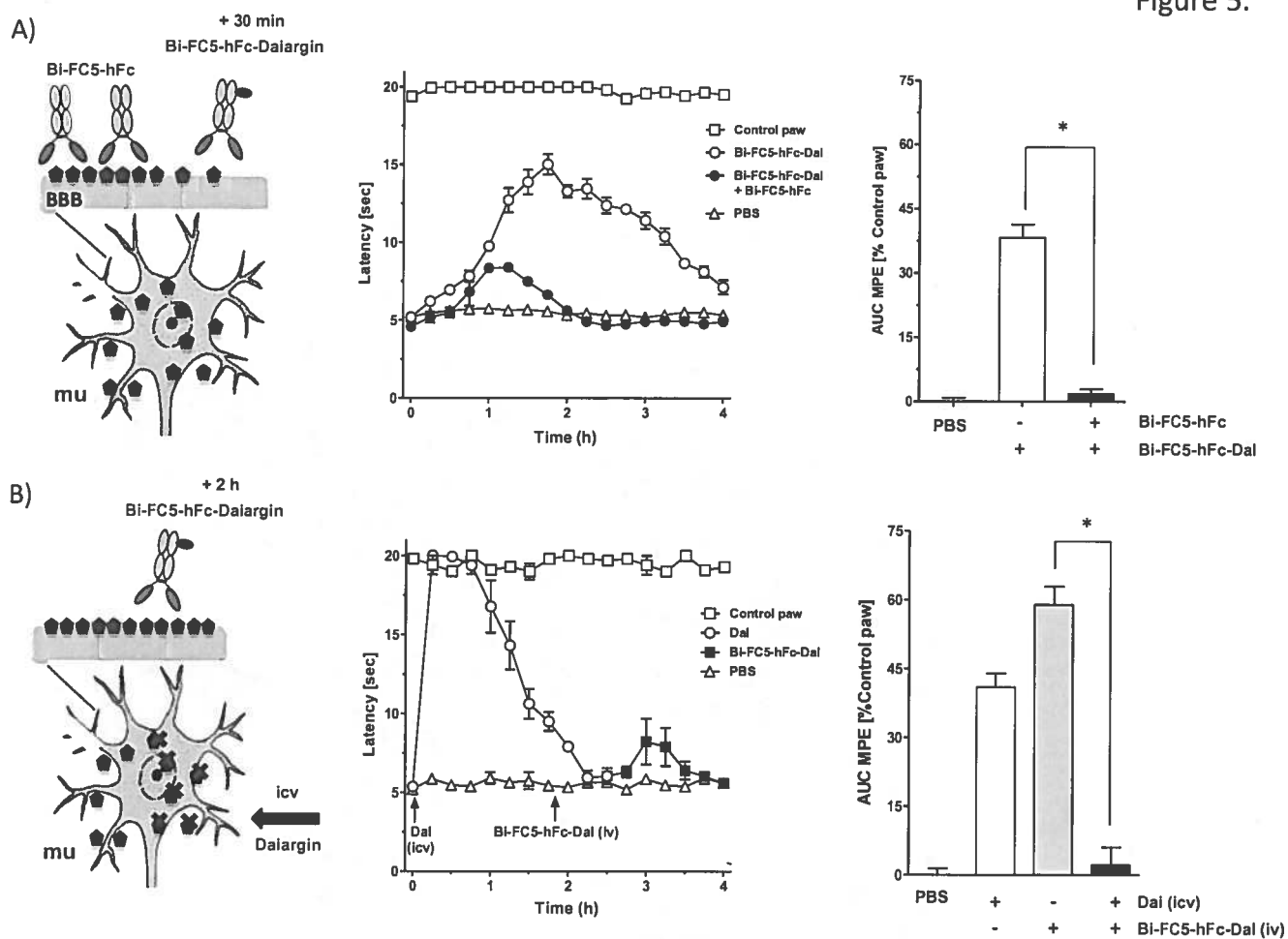
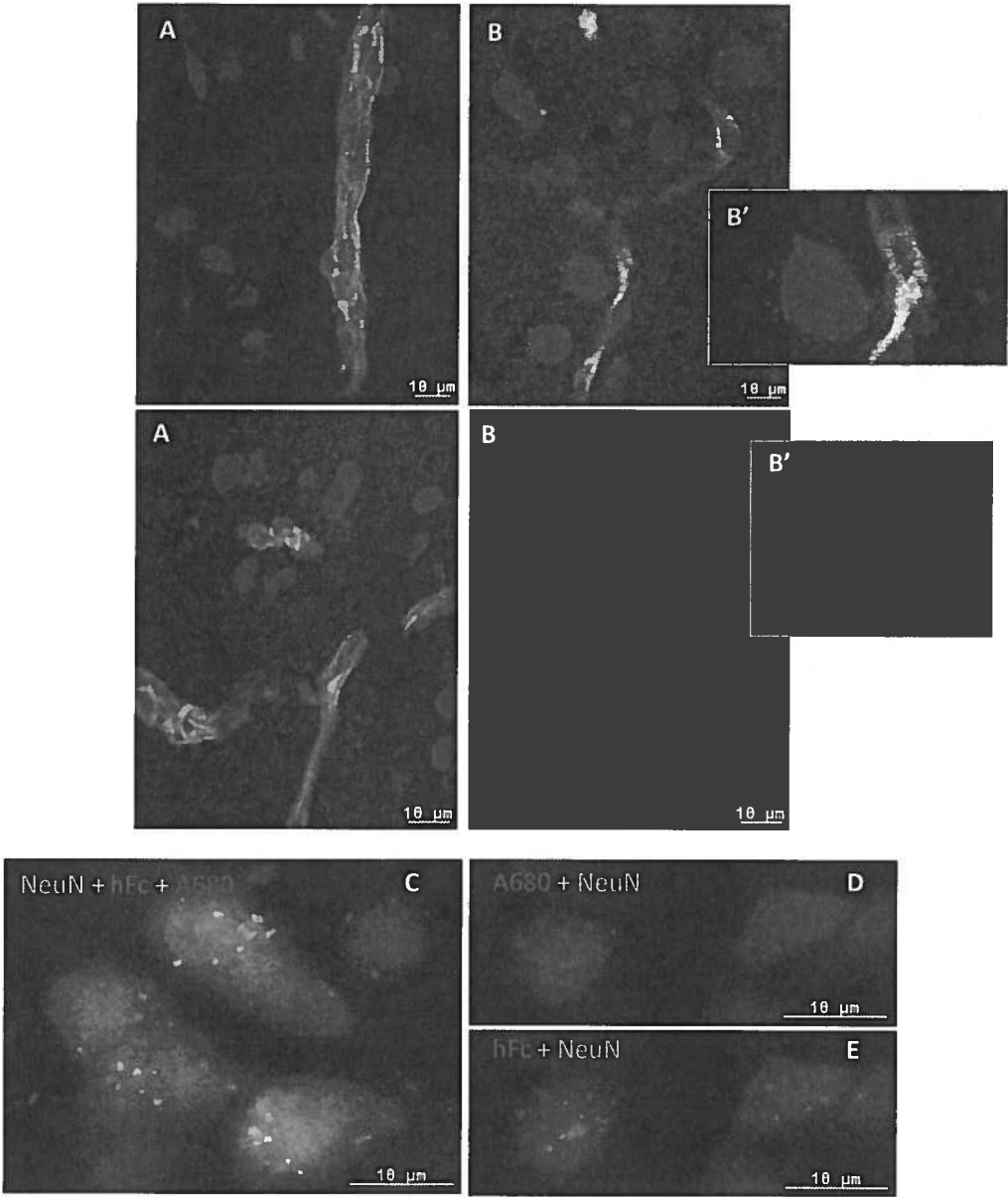
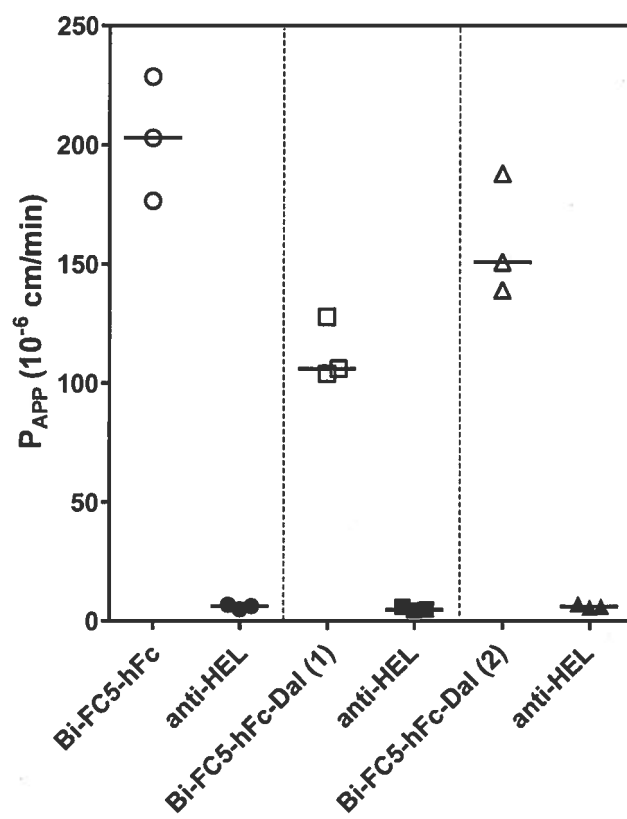


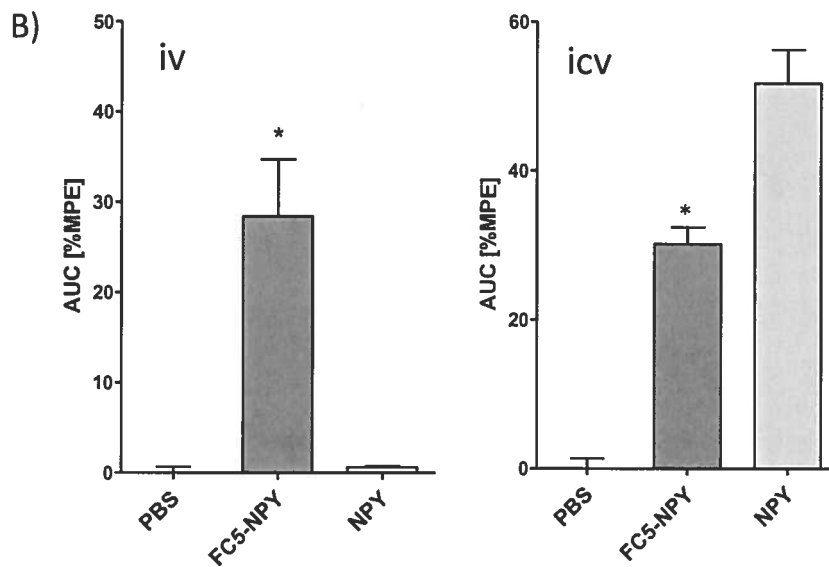
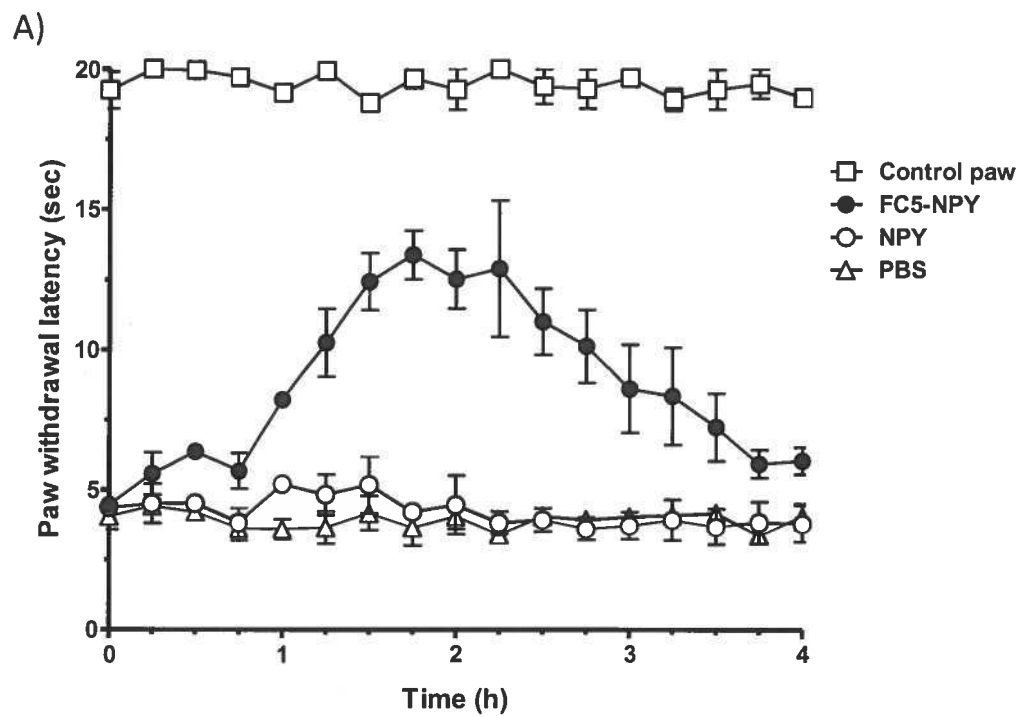
Figure 6.



Supplementary Figure S1.



Supplementary Figure S2.



Supplementary Figure S3.

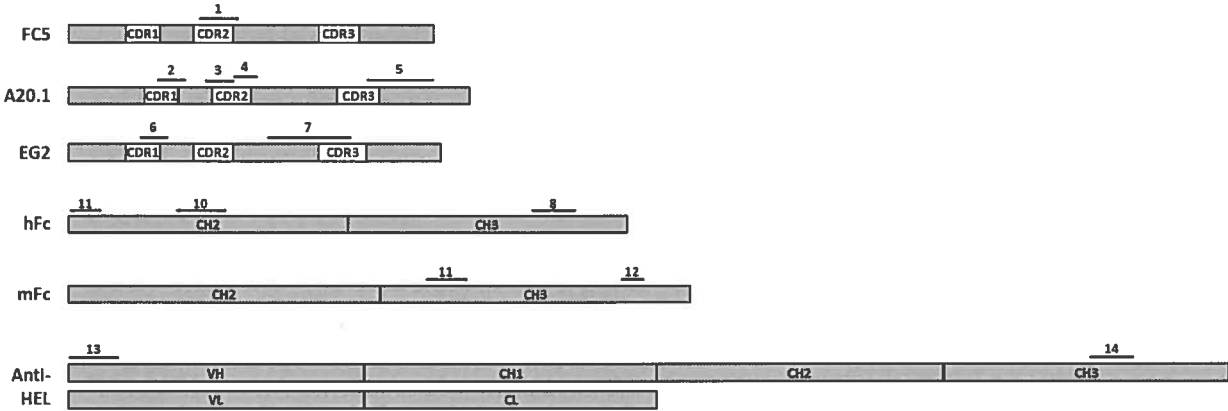


Table S1. In-line light scattering analysis and evaluation of average number of Dalargin peptides linked to each molecule. The number of conjugated Dalargin molecules was determined by MS from peaks eluting from gel filtration studies.

Molecule plasmid	FC5 ⁽¹⁾ (EAG2333)	Bi-FC5-hFc ⁽²⁾ (EAG2345)	Mono-FC5-hFc ⁽²⁾ (EAG2304)	hFc
Calculated Mwt (Daltons)	15,375	78,480	66,395	51,896
LS Mwt (Daltons)	15,980	77,530	78,950	57,800
Avg linked Dalargin peptides ⁽³⁾	1.5	1.5	1.5	1.0

(1) contains myc tag EQKLISEEDL, C-termini (1202 mwt), C-terminal His tag 5H

(2) Fc domains are human IgG1 and agly (all Fc domains contain a T299A point mutation in the hIgG sequence to eliminate Fc N-glycosylation)

(3) evaluated by MS, to determine the average number of Dalargin molecules covalently linked to the FC5-hFc domains.

Supplementary Figure S1.

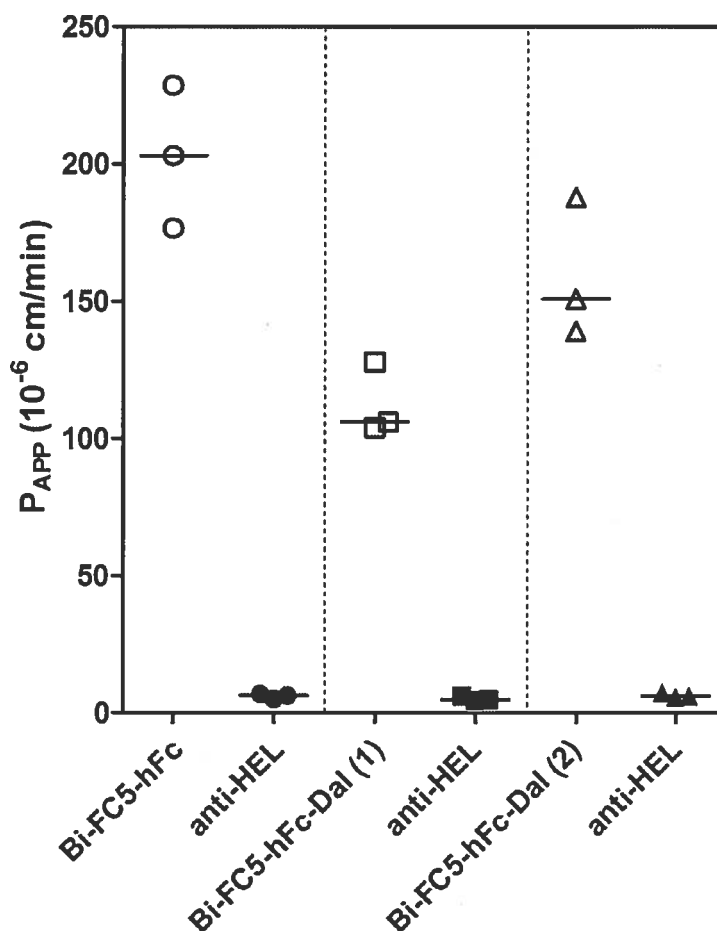


Fig S1. Effect of Dalargin cross-linking on Papp values of Bi-FC5-hFc. Two batches (1) and (2) of Bi-FC5-hFc-Dalargin conjugate show a 50% and 30% reduction in Papp values, respectively, compared to unconjugated Bi-FC5-hFc. Anti-HEL IgG was used as the internal control in each insert. Each point represents a Papp value derived from a separate insert. Bi-FC5-hFc-Dal conjugates showing Papp range of 150-200 cm/min were used in subsequent *in vivo* studies.

Supplementary Figure S2.

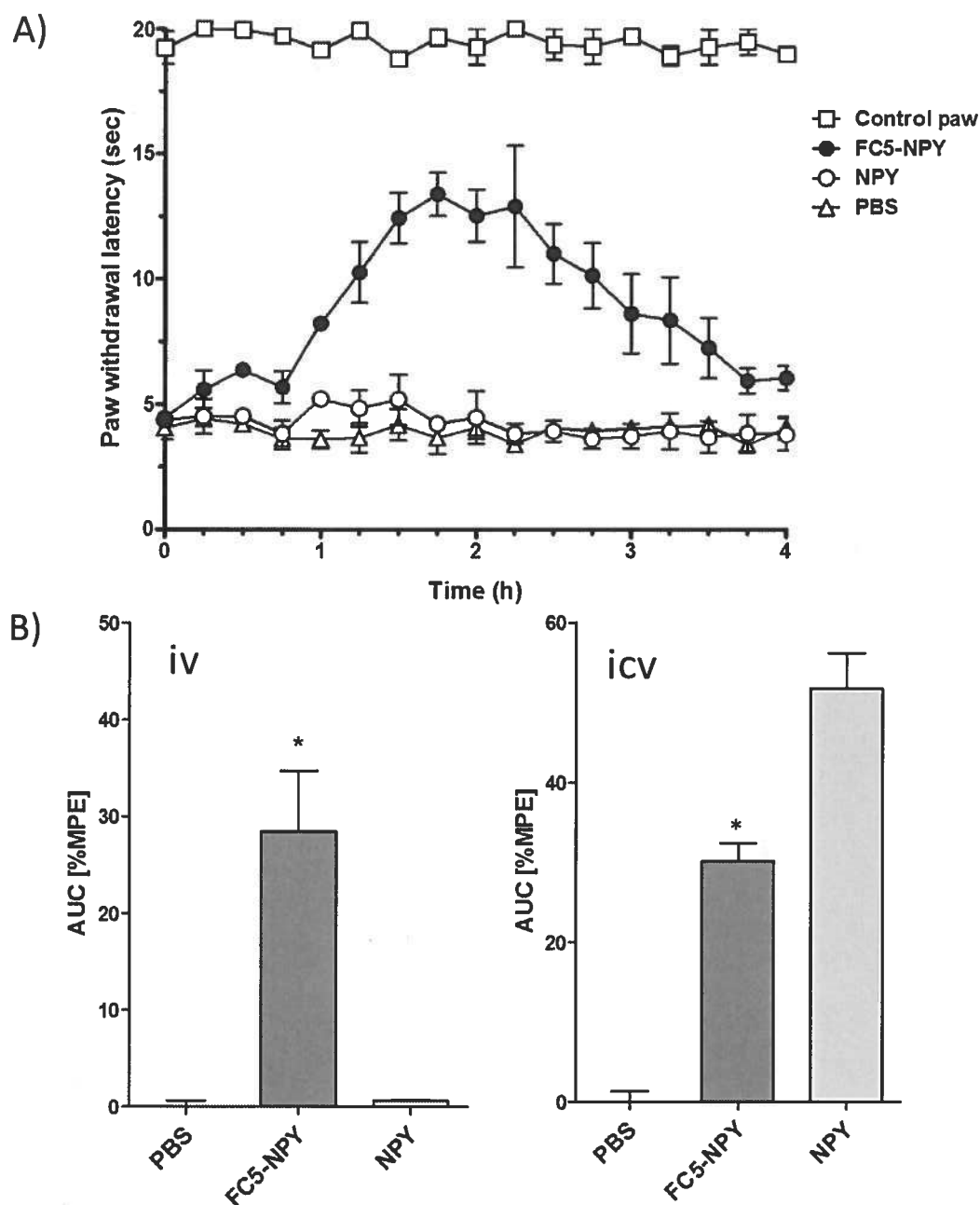


Fig S2. Effects of neuropeptide Y (NPY) chemically conjugated to FC5 on thermal hyperalgesia in Hargreaves model of inflammatory pain. A) Latency of withdrawal of control intact paw (open squares) or inflamed paw to a thermal stimulus was measured after two doses of PBS (500 μ l each) (open triangles) or NPY (2.02 mg/kg each) (open circles) or FC5-NPY (6.6 mg/kg each) (closed circles) given one hour apart (time 0 and 1 h). Data are shown as means \pm SD for 3-4 separate animals in each group. **B)** Analgesic effect achieved after either iv or icv administration of PBS, NPY and FC5-NPY shown as the integrated AUC over the duration of response (4h) expressed as percent MPE (control paw) (mean \pm SD of 3-6 animals in each group). For central effect, the rats received one icv injection of 2.5 μ g NPY or 93 μ g FC5-NPY. * - indicates statistical difference ($p < 0.01$; ANOVA) from NPY.

Supplementary Figure S3.

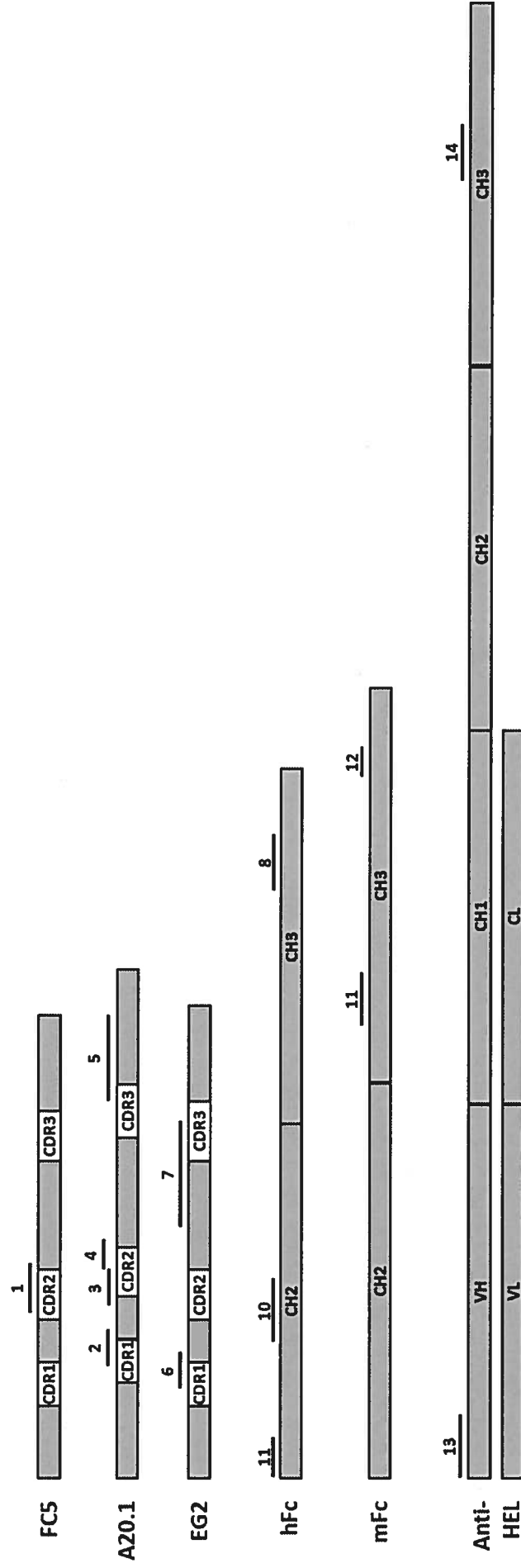


Fig S3. Location of SRM signatures used for quantitative analyses of various VHHs and human and mouse Fc.